Some aspects of three-quark potentials

Oleg Andreev

L.D. Landau Institute for Theoretical Physics, Kosygina 2, 119334 Moscow, Russia
and Arnold Sommerfeld Center for Theoretical Physics, LMU-München,
Theresienstrasse 37, 80333 München, Germany

We analytically evaluate the expectation value of a baryonic Wilson loop in a holographic model of an $SU(3)$ pure gauge theory. We then discuss three aspects of a static three-quark potential: an aspect of universality which concerns properties independent of a geometric configuration of quarks, a heavy diquark structure, and a relation between the three- and two-quark potentials.

I. INTRODUCTION

For many years, there has been great interest in triply heavy baryons [1,2]. The challenge here is to reach the level of knowledge similar to that of charmonium and bottomonium. On the theoretical side, the challenge is to explain the structure and properties of such baryons. It is expected that the potential models would be useful in doing so. Furthermore, in the process, one would expect to gain important insights into understanding how baryons are put together from quarks.

The three-quark potential is one of the most important inputs of the potential models and also a key to understanding the quark confinement mechanism in baryons. However, so far, there is no reliable formula to describe the three-quark potential. The best known phenomenological models are Ansätze which are a kind of Cornell model for a three-quark system. The Δ law states that the static three-quark potential is a sum of two-quark potentials [3].[1] In practice, it is taken to be the sum of Cornell-type potentials,

$$E_{3_Q}(\mathbf{x}_1, \mathbf{x}_2, \mathbf{x}_3) = \sum_{i<j}^{3} -\frac{\alpha_{3_Q}}{|\mathbf{x}_{ij}|} + \frac{1}{2}\sigma|\mathbf{x}_{ij}| + C, \qquad (1.1)$$

where $\mathbf{x}_i$ is the position vector of the ith quark, $\mathbf{x}_{ij} = \mathbf{x}_i - \mathbf{x}_j$, α_{3_Q} and C are parameters, and σ is the string tension. The relation with the quark-antiquark potential implies that $\alpha_{3_Q} = \frac{1}{2}\alpha_{Q\bar{Q}}$. The Δ law predicts that the energy grows linearly with the perimeter of the triangle formed by quarks. Alternatively, the Y law states that the energy grows linearly with the minimal length of a string network which has a junction at the Fermat point of the triangle [4–6]. In this case, a slight modification of (1.1) is of common use in the potential models. It is simply

$$E_{3_Q}(\mathbf{x}_1, \mathbf{x}_2, \mathbf{x}_3) = \sum_{i<j}^{3} -\frac{\alpha_{3_Q}}{|\mathbf{x}_{ij}|} + \sigma L_{\min} + C. \quad (1.2)$$

Unfortunately, there have not yet been any experimental results concerning triply heavy baryons. Thus, the predictions[2] based on either the Δ law or the Y law cannot be compared to the real world, and the last word has not yet been said on this matter. In such a situation, lattice gauge theory is the premier method for obtaining quantitative and nonperturbative predictions from strongly interacting gauge theories. The three-quark potentials are being studied on the lattice [8]. Although the accuracy of numerical simulations has been improved, the situation is still not completely clear. There is no problem with the fit by the Y law at long distances [9–11]. At shorter distances, the conclusion is mixed in the sense that some results favor the Δ law [10,12] and others favor the Y law [9,11,13].

The situation is even worse with the hybrid three-quark potentials. So far, there are no phenomenological predictions, and very little is known about those from lattice studies.[3] These potentials remain almost unknown and therefore merit more attention, as in the case of the hybrid quark-antiquark potentials [8,15].

One of the implications of the AdS/CFT correspondence [16] is that it opened a new window for studying strongly coupled gauge theories and, as a result, resumed interest in finding a string description (string dual) of QCD. It is worth noting that it is not an old fashioned four-dimensional string theory in Minkowski space but a five-(ten-)dimensional one in a curved space.

In this paper, we continue a series of studies [17,18] devoted to the three-quark potentials within a five- (ten-) dimensional effective string theory. The model we are developing represents a kind of soft wall model of Ref. [19], where the violation of conformal symmetry is manifest in the background metric [20]. It would be unwise to pretend that such a model is dual to QCD or that it can be deduced starting from the AdS/CFT correspondence. Our reasons for now pursuing this model are as follows:

---

[1]For more details, see Appendix D.

[2]For a recent development, see, e.g., Ref. [7].
[3]See, however, Ref. [14].

(1) There still is no string theory which is dual to QCD. It would seem very good to gain what experience we can by solving any problems that can be solved with the effective string model already at our disposal. The AdS/CFT correspondence is a good starting point because we already know a lot about Wilson loops in $\mathcal{N} = 4$ supersymmetric Yang-Mills theory [21].[4]

(2) The results provided by this model are consistent with the lattice calculations and QCD phenomenology. In some cases, the quantitative agreement is so good that one could not even expect such a success from a simple model. In Ref. [22], we have computed the quark-antiquark potential. Subsequent work made it clear that the model should be taken seriously, particularly in the context of consistency with the lattice [23] and quarkonium spectrum [24]. Another instance of perfect consistency between the model [18] and the lattice calculations [9,11,12] is the three-quark potential obtained on an equilateral triangle. In addition, the model also reproduces one of the hybrid potentials of Ref. [25]. It is the Σ_u^- potential [26].

(3) Analytic formulas are obtained by solving the model. This allows one to easily compare the results with the lattice and QCD phenomenology.

(4) The model is able to explore QCD properties in the transition region between confinement and asymptotic freedom. As seen from Fig. 3, it can operate at length scales down to 0.2 fm. This is a big advantage of the model over any type of old fashioned four-dimensional string model in Minkowski space.

(5) The aim of our work is to make predictions which may then be tested by means of other methods, e.g., numerical simulations.

Of course, it is worth keeping in mind that this model, as any other model, has its own limitations. In particular, it breaks down at very small length scales, which makes it impossible to compare the results with those of perturbative QCD.

The paper is organized as follows. For orientation, we begin by setting the framework and recalling some preliminary results. Then, we consider the three-quark potential of collinear quarks. This allows us to compare the results with those obtained on the equilateral geometry and make predictions on what is expected to be universal (independent of a geometrical configuration of quarks) at short and long distances. We go on in Sec. III to discuss the quark-diquark and quark-quark potentials as the limiting cases of that obtained for the collinear geometry. Our goal here is to determine the leading terms in the interquark

potential. In Sec. IV, we give an example of the three-quark hybrid potential. Here, we also consider a relation between two and three hybrid quark potentials and make a prediction of universality for a gap between the potential and its hybrid at long distances. We conclude in Sec. V with a discussion of some open problems and possibilities for further study. Some technical details are given in the Appendixes.

II. THREE-QUARK POTENTIAL VIA GAUGE/STRING DUALITY

In this section, we will derive the three-quark potential for two different geometries. We start with an equilateral triangle geometry and then consider a collinear geometry. Although we mainly concentrate on the collinear geometry, as our basic example, the approach is equally applicable for any geometry. Appendixes A and B provide the necessary tool kit for doing so.

A. Preliminaries

The static three-quark potential can be determined from the expectation value of a baryonic Wilson loop [8]. The Wilson loop in question is defined in a gauge-invariant manner as $W_{3Q} = \frac{1}{3!}\varepsilon_{abc}\varepsilon_{a'b'c'}U_1^{aa'}U_2^{bb'}U_3^{cc'}$, with U_i the path-ordered exponents along the lines shown in Fig. 1. In the limit $T \to \infty$, the expectation value of W_{3Q} is given by

$$\langle W_{3Q} \rangle = \sum_{n=0}^{\infty} B_n e^{-E_{3Q}^{(n)}T}. \qquad (2.1)$$

Here, $E_{3Q}^{(0)}$ is called the three-quark potential (ground-state energy) if the corresponding contribution dominates the sum as T approaches infinity. In other words, it requires $E_{3Q}^{(0)} < E_{3Q}^{(i)}$ for any $i > 0$ and any quark configuration. If so, then the remaining $E_{3Q}^{(i)}$'s are called hybrid three-quark potentials (excited-state energies).
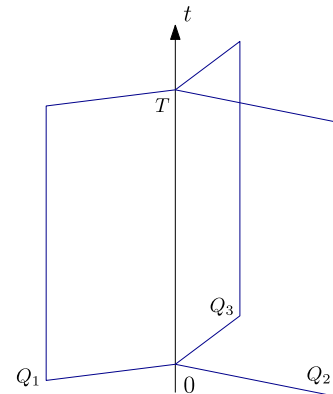

FIG. 1. A baryonic Wilson loop. A three-quark state $Q_1Q_2Q_3$ is generated at $t = 0$ and is annihilated at $t = T$.

---

[4]There is an obvious question. If $N = 3$, why is it a good starting point? We have no answer and take this as an assumption, but (2) partially resolves the question.

In our study of baryonic Wilson loops, we adapt a formalism proposed within the AdS/CFT correspondence [27,28] to a confining gauge theory.

First, we take the Ansatz for the background metric

$$ds^2 = e^{\mathfrak{s}r^2}\frac{R^2}{r^2}(dt^2 + d\vec{x}^2 + dr^2) + e^{-\mathfrak{s}r^2}g^{(5)}_{ab}d\omega^a d\omega^b. \tag{2.2}$$

Thus, the geometry in question is a one-parameter deformation, parametrized by $\mathfrak{s}$, of a product of a five-dimensional (Euclidean) anti–de Sitter space (AdS$_5$) of radius R and a five-dimensional compact space (sphere) **X** of which the coordinates are ω^a. In Eq. (2.2), there are the two free parameters R and $\mathfrak{s}$. Note that the first combines with α' from the Nambu-Goto action (A1) such that $\mathfrak{g} = \frac{R^2}{2\pi\alpha'}$ then is to be fitted. Since we deal with an effective string theory based on the Nambu-Goto formulation,[5] knowing the background geometry is sufficient for our purposes. There are good motivations for taking this Ansatz. First, such a deformation of AdS$_5$ leads to linear Regge-like spectra for mesons [19,20] and the quark-antiquark potential [22], which is very satisfactory in the light of lattice gauge theory and phenomenology [23,24]. Second, the deformation of **X** is motivated by thermodynamics [29].

Next, we consider the baryon vertex. In the static gauge, we take the Ansatz

$$S_{\text{vert}} = m\frac{e^{-2\mathfrak{s}r^2}}{r}T \tag{2.3}$$

for its action, where m and $\mathfrak{s}$ are parameters. Note that the parameter $\mathfrak{s}$ is the same as in Eq. (2.2) so that only m is a new one.

In what follows, we will assume that quarks are placed at the same point in the internal space.[6] Therefore, the detailed structure of **X** is not important, except the exponential warp factor depending on the radial direction. The motivation for such a form of the warp factor is drawn from the AdS/CFT construction, where the baryon vertex is a 5-brane [27]. Taking a term $\int dt d^5\omega\sqrt{g^{(6)}}$ from the world volume action of the brane results in $Te^{-2\mathfrak{s}r^2}/r$. This is, of course, a heuristic argument, but it leads to the very satisfactory result that the lattice data of [9,11,12] obtained on an equilateral triangle can be described by a single parameter [18].

One of the important differences between QCD and AdS/CFT is that QCD has gotten much further than AdS/CFT in addressing the issue of hybrid potentials [15]. The common wisdom is that those potentials correspond to excited strings [5]. The structure of string excitations is quite complicated and is made of many different kinds of elementary excitations like vibrational modes, loops, knots, etc. Adopting the view point that some excitations imply a formation of cusps, one can model them by inserting local objects (defects) on a string.[7] Thus, what we need is an action for such an object. In the static gauge, we take the action to be of the form

$$S_{\text{def}} = n\frac{e^{-2\mathfrak{s}r^2}}{r}T, \tag{2.4}$$

where n and $\mathfrak{s}$ are parameters. Again, $\mathfrak{s}$ is the same as in Eq. (2.2).

The form like (2.4) seems natural if one thinks of the defect as a tiny loop formed by a pair of baryon-antibaryon vertices connected with fundamental strings. In such a scenario, the expression (2.4) is based on an assumption that the strings do not change the radial dependence in (2.3). This is also a heuristic argument, but it can be confronted with the lattice data of [25]. For Σ_u^-, the result is in good agreement [26]. Notice that (2.4) contains only one free parameter that makes it attractive from the phenomenological point of view.

Finally, we place heavy quarks at the boundary points of the five-dimensional space ($r = 0$) but at the same point in the internal space **X**. We consider configurations in which each quark is the end point of the Nambu-Goto string, with the strings joining at the baryon vertex in the interior as shown in Fig. 2. For excited strings, we also place defects on them as shown in Fig. 8. The total action of a system has, in addition to the standard Nambu-Goto actions, also contributions arising from the baryon vertex and defect. The expectation value of the Wilson loop is then

$$\langle W_{3_Q} \rangle \sim e^{-S_{\min}}, \tag{2.5}$$

where $S_{\min}$ is the minimal action of the system. Combining it with (2.1) gives the three-quark potential.[8]

B. Equilateral triangle geometry

As a warmup, let us give a derivation of the three-quark potential in the case in which the quarks are at the vertices of an equilateral triangle of length L [18]. To this end, we

---

[5]This has some limitations. The reason is that the Green-Schwarz formulation similar to that for AdS$_5 \times$ **S**^{5} is still missing. So, we consider the model as an effective theory rather than an ultimate solution for QCD.

[6]It is worth noting that this assumption makes the problem effectively five dimensional and hence more tractable. From the five-dimensional point of view, the vertex looks like a pointlike object (particle).

---

[7]A similar idea was used in four-dimensional string models, but with a different goal, such as a description of linear baryons. For more discussion and references, see Ref. [30].

[8]Like in AdS/CFT, this formula is oversimplified for various reasons, but it seems acceptable for the purposes of the effective string theory based on the Nambu-Goto formulation.
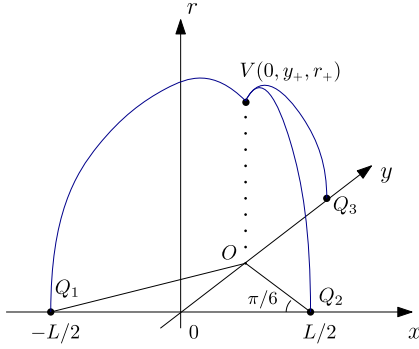
FIG. 2.   A baryon configuration. The quarks Q_i are placed at the vertices of the equilateral triangle. V is a baryon vertex.

consider the configuration shown in Fig. 2. Here, gravity pulls the baryon vertex toward the boundary that allows the result to be consistent with the lattice data [9–12].

The D_3 symmetry of the problem immediately implies that the projection of V onto the xy plane is a center of the triangle and all the strings have an identical profile. In this case, a radius of the circumscribed circle is given by (A16), and as a consequence, the triangle's side length is[9]

$$L = \sqrt{\frac{3\lambda}{\mathfrak{s}}}\left[\int_0^1 dv v^2 e^{\lambda(1-v^2)}(1 - v^4 e^{2\lambda(1-v^2)})^{-\frac{1}{2}}\right.$$
$$\left. + \int_{\sqrt{\frac{\nu}{\lambda}}}^1 dv v^2 e^{\lambda(1-v^2)}(1 - v^4 e^{2\lambda(1-v^2)})^{-\frac{1}{2}}\right], \quad (2.6)$$

where $\lambda \in [0, 1]$ and $\nu \leq \lambda$. Note that $\nu = \mathfrak{s}r_+^2$ and $\lambda = \mathfrak{s}r_{\max}^2$, with $r_{\max}$ shown in Fig. 10.

It is straightforward to compute the total energy of the configuration $E = \sum_{i=1}^3 E_i + \mathcal{V}(r_+)$. The energy of a single string is given by Eq. (A20). Then, using this expression and the expression (2.3) for the gravitational energy of the baryon vertex, we find

$$E_{3Q} = 3\mathfrak{g}\sqrt{\frac{\mathfrak{s}}{\lambda}}\left[\kappa\sqrt{\frac{\lambda}{\nu}}e^{-2\nu} + \int_0^1 \frac{dv}{v^2}(e^{\lambda v^2}(1 - v^4 e^{2\lambda(1-v^2)})^{-\frac{1}{2}}\right.$$
$$\left. - 1 - v^2) + \int_{\sqrt{\frac{\nu}{\lambda}}}^1 \frac{dv}{v^2}e^{\lambda v^2}(1 - v^4 e^{2\lambda(1-v^2)})^{-\frac{1}{2}}\right] + C,$$
$$(2.7)$$

with C a normalization constant. It is equal to $3c$ as it follows from Eq. (A20). In addition, $\kappa = \frac{m}{3\mathfrak{g}}$, as defined in Eq. (B10).

At this point, we can complete the parametric description of the three-quark potential for the equilateral triangle geometry. To this end, the gluing conditions at the vertex should be involved. When the triangle is equilateral, we impose the condition (B10)

$$\sin\alpha = \kappa(1 + 4\nu)e^{-3\nu}, \quad (2.8)$$

which is nothing else but the balance of force in the radial direction. Here, we have abbreviated α_+ to α. Note that a negative value of α, as sketched in Fig. 2, implies that $\kappa < 0$. In this case, the gravitational force is directed in the downward vertical direction.

Combining Eq. (2.8) with Eq. (A18), one can express λ in terms of the ProductLog function [31]

$$\lambda(\nu) = -\text{ProductLog}[-\nu e^{-\nu}(1 - \kappa^2(1 + 4\nu)^2 e^{-6\nu})^{-\frac{1}{2}}].$$
$$(2.9)$$

Here, $\nu \in [0, \nu_*]$, with ν_* a solution to $\lambda(\nu) = 1$.

Thus, the potential is given in parametric form by $E_{3Q} = E(\nu)$ and $L = L(\nu)$. The parameter takes values on the interval $[0, \nu_*]$. This is the main result of this section. It is a special case of the result announced in Ref. [18].

Now, we wish to compare this result to the lattice data and see some of the surprising features of our model. But first let us look at the behavior of $E_{3Q}(L)$ at short and long distances.

A simple analysis shows that $L(\nu)$ is a monotonically increasing function on the interval $[0, \nu_*]$ and that $L(\nu)$ goes to zero as $\nu \to 0$ and goes to infinity as $\nu \to \nu_*$. Thus, to analyze the short distance behavior of E_{3Q}, we need to find the asymptotic behavior of $L(\nu)$ and $E(\nu)$ near $\nu = 0$.[10] In this case, we restrict ourselves to the two leading terms, which allow us to easily obtain the energy as a function of the triangle's side length. Thus, at short distances, the three-quark potential is given by

$$E_{3Q}(L) = -3\frac{\alpha_{3Q}}{L} + C + \frac{3}{2}\sigma_0 L + o(L), \quad (2.10)$$

with

$$\alpha_{3Q} = -\frac{1}{3}L_0 E_0 \mathfrak{g}, \quad \sigma_0 = \frac{2}{3L_0}\left(E_1 + \frac{L_1}{L_0}E_0\right)\mathfrak{g}\mathfrak{s}. \quad (2.11)$$

The L_i's and E_i's are expressed in terms of the beta function and given by Eqs. (C3) and (C4), respectively.

In a similar spirit, we can explore the long distance behavior of E_{3Q}. Expanding the right-hand sides of Eqs. (2.6) and (2.7) near $\nu = \nu_*$, we reduce these equations to a single equivalent equation,

$$E_{3Q}(L) = \sqrt{3}\sigma L + \mathfrak{c} + o(1), \quad (2.12)$$

with

---

[9]We abbreviate ν_+ to ν when this is not ambiguous.
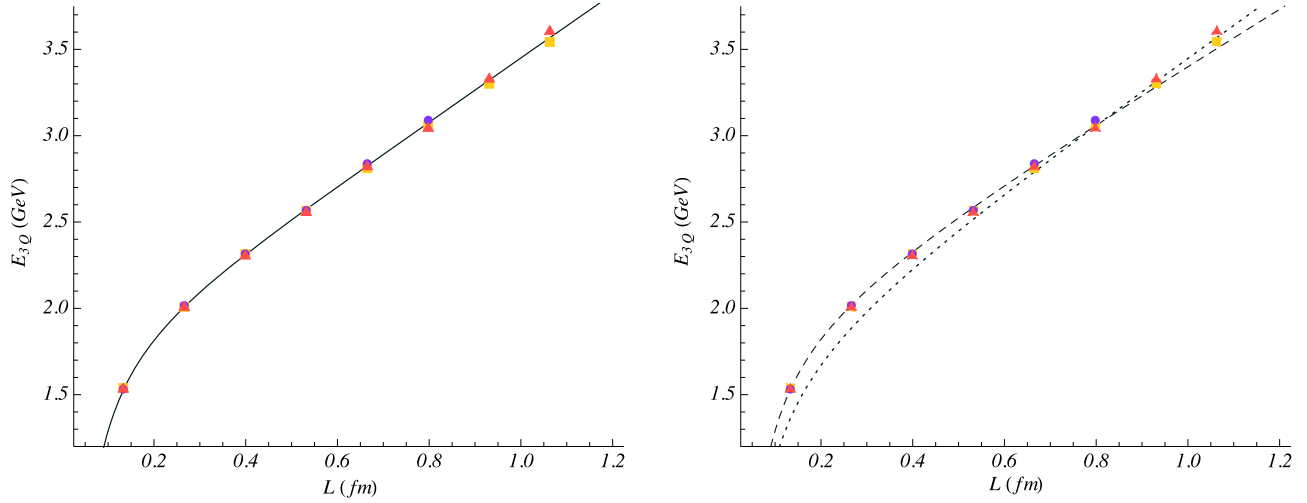
[10]For details, see Appendix C.

FIG. 3.   The lattice data are taken from Refs. [10,12] (squares), [9] (disks), and [11] (triangles). We use the normalization of [12]. We do not display any error bars because they are comparable to the size of the symbols. Left: E_{3_Q} as a function of L at $\mathfrak{g} = 0.176$, $\mathfrak{s} = 0.44$ GeV^2, $\kappa = -0.083$, and $C = 1.87$ GeV. Right: The Δ law (2.10) (dashed) and the Y law (2.18) (dotted).

$$\sigma = e\mathfrak{g}\mathfrak{s},$$

$$c = 3\mathfrak{g}\sqrt{\mathfrak{s}}\left[\frac{\kappa}{\sqrt{\nu_*}}e^{-2\nu_*} + \int_0^1 \frac{dv}{v^2}\left(e^{v^2}(1-v^4 e^{2(1-v^2)})^{\frac{1}{2}}\right.\right.$$

$$\left.\left. - 1 - v^2\right) + \int_{\sqrt{\nu_*}}^1 \frac{dv}{v^2} e^{v^2}(1-v^4 e^{2(1-v^2)})^{\frac{1}{2}}\right] + C.$$

$$(2.13)$$

Here, σ is the physical string tension. It remains universal and unaltered in all the cases: the quark-antiquark [22], hybrid [26], three-quark potentials [17], and also in the examples we consider below. It is notable that the constant terms at short and long distances are different. Because of scheme ambiguities, each of those has no physical meaning, but the difference

$$c - C = 3\mathfrak{g}\sqrt{\mathfrak{s}}\left[\frac{\kappa}{\sqrt{\nu_*}}e^{-2\nu_*} + \int_0^1 \frac{dv}{v^2}\left(e^{v^2}(1-v^4 e^{2(1-v^2)})^{\frac{1}{2}}\right.\right.$$

$$\left.\left. - 1 - v^2\right) + \int_{\sqrt{\nu_*}}^1 \frac{dv}{v^2} e^{v^2}(1-v^4 e^{2(1-v^2)})^{\frac{1}{2}}\right] \quad (2.14)$$

is not ambiguous and is free from divergences. This makes the model so different from the phenomenological laws (1.1) and (1.2), where the difference vanishes.

Having found the asymptotic behaviors at short and long distances, we can compare our model of the three-quark potential with the results of numerical simulations. We proceed along the lines of Ref. [18]. First, we set $\mathfrak{g} = 0.176$ and $\mathfrak{s} = 0.44$ GeV^2, i.e., to the same values as those of Ref. [26] used for modeling the quark-antiquark potentials of [25]. Then, the remaining parameter is fitted to be $\kappa = -0.083$ using the data of Ref. [12] from numerical simulations of the baryonic Wilson loops. The result is

plotted in Fig. 3. We see that the model reproduces the lattice data remarkably well with just one free parameter.

A simple estimate using Eq. (2.11) and the fitted value of κ shows that [18]

$$\frac{\alpha_{3_Q}}{\alpha_{Q\bar{Q}}} \approx 0.495, \qquad \frac{\sigma_0}{\sigma} \approx 1.007, \qquad (2.15)$$

where $\alpha_{Q\bar{Q}}$ is a coefficient in front of the Coulomb term of the quark-antiquark potential [22]. Explicitly, it is given by $\alpha_{Q\bar{Q}} = (2\pi)^3 \Gamma^{-4}(\frac{1}{4})\mathfrak{g}$ [32]. This suggests that at short distances Eq. (2.10) can be rewritten as

$$E_{3_Q}(L) \approx -\frac{3}{2}\frac{\alpha_{Q\bar{Q}}}{L} + C + \frac{3}{2}\sigma L + o(L) \approx \frac{1}{2}\sum_{i<j}^3 E_{Q\bar{Q}}(r_{ij}),$$

$$(2.16)$$

where $E_{Q\bar{Q}}(r_{ij})$ is the quark-antiquark potential and r_{ij} denotes the distance between the vertices i and j. With our choice of normalization, the normalization constant C for the energy of a single baryon configuration is equal to $3c$, while that of the quark-antiquark pair is $2c$ [see Eq. (A23)]. This is consistent with the relation (2.16). Actually, it is the Δ law suggested in Ref. [3]. The analysis of Refs. [10,12,18] shows that it is a good approximation to the lattice at distances shorter than 0.6–0.8 fm.

The underlying physical picture is not necessarily very accurate for baryons. We suggest that the Δ law can be treated in a way that helps clarify the physics of strong interactions and at the same time complies with the lattice. The picture that emerges from this point of view is that at short distances the three-quark potential is described by a

sum of two-body potentials. At length scales where a diquark can be treated as a pointlike object, it is simply

$$E_{3_Q}(L) \approx \frac{1}{2}\sum_{i<j}^{3} E_{QD}(r_{ij}), \qquad (2.17a)$$

with E_{QD} a quark-diquark potential. This is plausible because in this case E_{QD} coincides with the quark-antiquark potential such that (2.17a) reduces to Eq. (2.16). Alternatively, it may be written as a sum over all quark-quark pairs,

$$E_{3_Q}(L) \approx \sum_{i<j}^{3} E_{QQ}(r_{ij}), \qquad (2.17b)$$

with E_{QQ} a quark-quark potential. Notice that (2.17b) can be derived from (2.16) by using the one-half rule $E_{QQ} \approx \frac{1}{2} E_{Q\bar{Q}}$ [2]. We will return to these issues again in Sec. III and Appendix D.

Actually, in connection with the above analysis, some additional questions should be asked. To reach the conclusion that in the interval [0.2 fm, 0.7 fm] the three-quark potential is well approximated by a sum of two-body potentials, we analyzed the short distance behavior of the expressions (2.6) and (2.7). It turns out that the first terms of the series (2.10) provide a good approximation in this interval, as can be seen from Fig. 3. This is a model artifact. Does it imply that (2.10) is also reliable at shorter distances? This is unclear. Certainly, no resummation of perturbative series of a pure $SU(3)$ gauge theory is known. But it might occur that resummation will lead to the form of Eq. (2.10). In addition, the relation (2.15) between $\alpha_{Q\bar{Q}}$ and α_{3_Q} is similar to that of the tree-level result. What may be the reason? In the model we are considering, α_{3_Q} is a function of the parameter κ, while $\alpha_{Q\bar{Q}}$ is a constant. So, there may be any relation between those coefficients. The peculiar one is the result of fitting to the lattice. Again, to really explain why it is so, resummation of perturbative series is needed.

What happens at longer distances? We can reasonably expect that Eq. (2.12) is a proper approximation for E_{3_Q}. This is indeed the case [18]. It is interesting that the Lüscher correction to Eq. (2.12) turns out to be negligible. In fact, such a behavior is also provided by the Y law at long distances [4,5].

Thus, the physical picture we have is that our model incorporates two-body interactions, the Δ law, at short distances and a genuine three-body interaction, the Y law, at longer distances. In the string context, the two-body interaction is described by a single string stretched between a quark and a diquark, while the three-body interaction is the standard one. It includes three strings meeting at a common junction. Mathematically, $E_{3_Q}(L)$ is a complicated

function of L of which the asymptotic behavior is described by the Δ and Y laws.

If one includes the Lüscher correction, like in the Y law,[11]

$$E_{3_Q}(L) = \sqrt{3}\sigma L + c_Y - 3\frac{\alpha_{3_Q}}{L}, \qquad (2.18)$$

then the whole picture does not change and remains the same as before, except the transition between the two behaviors occurs at a slightly larger scale, of order 0.8 fm as seen from Fig. 3.

So far, we have tacitly assumed that gravity pulls the vertex toward the boundary. This is an important difference between our model and those in the literature devoted to duals of large N (supersymmetric) gauge theories. There are obvious questions one can ask about what took place. Is the $1/N$ expansion really a good approximation? What is the origin for κ being negative? Is it a model artifact? Unfortunately, no real resolution of this problem will be proposed here. Our criterion is to mimic QCD and provide the basis for further calculations.

C. Symmetric collinear geometry

Given the set of parameters that we have just fitted, it is straightforward to determine the three-quark potential for other geometries and make some predictions in the cases when there are no lattice data available. To get some intuition, we first consider the symmetric collinear geometry.

As before, we place the quarks at the boundary points of the five-dimensional space and consider a configuration in which each of the quarks is the end point of a fundamental string. The strings join at a baryon vertex in the interior as shown in Fig. 4, on the left. For convenience, the quarks are on the x axis such that $x_1 = -L$, $x_2 = L$, and $x_3 = 0$.

Since the quark configuration is symmetric under reflection through $x = 0$, the side strings have an identical profile, and the middle string is stretched in the radial direction. Given this, we can use the general formula (A16) to write

$$L = \sqrt{\frac{\lambda}{\mathfrak{s}}} \left[\int_0^1 dv v^2 e^{\lambda(1-v^2)} (1 - v^4 e^{2\lambda(1-v^2)})^{-\frac{1}{2}} \right.$$
$$\left. + \int_{\sqrt{\frac{\nu}{\lambda}}}^1 dv v^2 e^{\lambda(1-v^2)} (1 - v^4 e^{2\lambda(1-v^2)})^{-\frac{1}{2}} \right], \qquad (2.19)$$

where $\nu = \mathfrak{s} r_+^2$ and $\lambda = \mathfrak{s} r_{\max}^2$, with $r_{\max}$ shown in Fig. 10.

The expression for the total energy can be read from the formulas (A10), (A20), and (2.3). We have

---

[11]This issue was raised by H. Suganuma. Here, we replace $c \approx 1.60$ GeV by $c_Y \approx 1.67$ GeV to better fit the data.
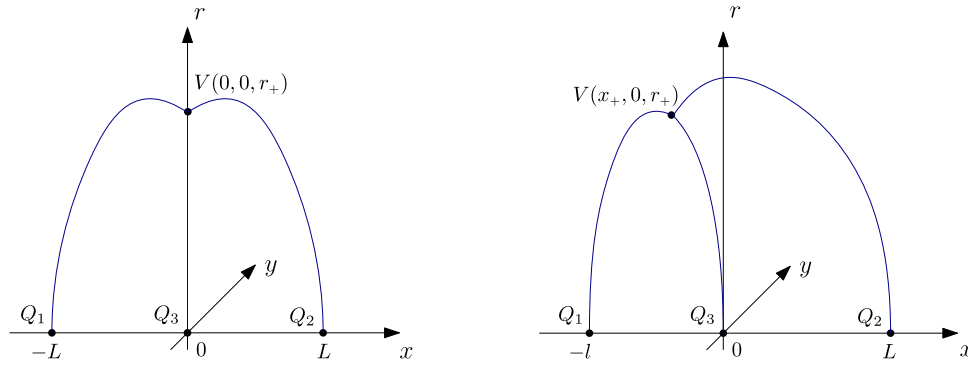
FIG. 4. Typical collinear configurations. Left: A symmetric configuration. Right: A generic configuration. Here, $l < L$.

$$E_{3_Q} = 2\mathfrak{g}\sqrt{\frac{\mathfrak{s}}{\lambda}}\left[\int_0^1 \frac{dv}{v^2}\left(e^{\lambda v^2}(1 - v^4 e^{2\lambda(1-v^2)})^{-\frac{1}{2}} - 1 - v^2\right)\right.$$

$$\left. + \int_{\sqrt{\frac{\xi}{\lambda}}}^1 \frac{dv}{v^2} e^{\lambda v^2}(1 - v^4 e^{2\lambda(1-v^2)})^{-\frac{1}{2}}\right]$$

$$+ \mathfrak{g}\sqrt{\frac{\mathfrak{s}}{\nu}}(\sqrt{\pi\nu}\,\mathrm{Erfi}(\sqrt{\nu}) - e^\nu + 3\kappa e^{-2\nu}) + C. \quad (2.20)$$

As before, the normalization constant is given by $C = 3c$.

A complete description has to include the gluing conditions at the vertex. Such conditions are given by Eq. (B12) with $\alpha_1 = \alpha_2 = \alpha$ and $\alpha_3 = \frac{\pi}{2}$. So, we have

$$2\sin\alpha + 1 = 3\kappa(1 + 4\nu)e^{-3\nu}. \quad (2.21)$$

It is convenient to express λ as a function of ν. By combining (2.21) and (A18), we get

$$\lambda(\nu) = -\mathrm{ProductLog}\left(-\frac{2}{\sqrt{3}}\nu e^{-\nu}(1 + 2\kappa(1 + 4\nu)e^{-3\nu}\right.$$

$$\left. - 3\kappa^2(1 + 4\nu)^2 e^{-6\nu})^{-\frac{1}{2}}\right). \quad (2.22)$$

In summary, the three-quark potential is given by the parametric equations (2.19) and (2.20). The parameter ν takes values in the interval $[0, \nu_\star]$, where $\lambda(\nu_\star) = 1$.

The analysis of $E_{3_Q}(L)$ in the two limiting cases, long and short distances, is formally similar to that of the previous section. The first step is to learn that $L(\nu)$ is an increasing function on the interval $[0, \nu_\star]$. Moreover, it goes from zero to infinity. Having learned this, we can obtain the short distance behavior by expanding $L(\nu)$ and $E(\nu)$ near $\nu = 0$ and then reducing the two equations to a single one,

$$E_{3_Q}(L) = -\frac{5}{2}\frac{\alpha_{3_Q}}{L} + C + 2\sigma_0 L + o(L), \quad (2.23)$$

where

$$\alpha_{3_Q} = -\frac{2}{5}L_0 E_0 \mathfrak{g}, \quad \sigma_0 = \frac{1}{2L_0}\left(E_1 + \frac{L_1}{L_0}E_0\right)\mathfrak{g}\mathfrak{s}. \quad (2.24)$$

The L_i's and E_i's are defined in Eqs. (C6) and (C7), respectively.

To analyze the long distance behavior, we expand the right-hand sides of Eqs. (2.19) and (2.20) near $\nu = \nu_\star$, then reduce these equations to

$$E(L) = 2\sigma L + \mathrm{c} + o(1), \quad (2.25)$$

where

$$\mathrm{c} = \mathfrak{g}\sqrt{\mathfrak{s}}\left[\sqrt{\pi}\,\mathrm{Erfi}(\sqrt{\nu_\star})\right.$$

$$+ 2\int_0^1 \frac{dv}{v^2}(e^{v^2}(1 - v^4 e^{2(1-v^2)})^{\frac{1}{2}} - 1 - v^2)$$

$$\left. + 2\int_{\sqrt{\nu_\star}}^1 \frac{dv}{v^2}e^{v^2}(1 - v^4 e^{2(1-v^2)})^{\frac{1}{2}} + \frac{3\kappa e^{-2\nu_\star} - e^{\nu_\star}}{\sqrt{\nu_\star}}\right] + C.$$

$$(2.26)$$

$\mathrm{Erfi}(x)$ denotes the imaginary error function. As before, the constant terms C and c turn out to be different.

Now, we wish to make some predictions. Otherwise, this will remain as an academic exercise in gauge/string duality. So far, there are no lattice data available for the symmetric collinear geometry, and therefore we compare the results with the phenomenological Ansätze and those from the previous section.

In Fig. 5, we display the three-quark potential obtained from Eqs. (2.19) and (2.20). Because the phenomenological Δ and Y laws coincide for the collinear configuration, one could expect that the potential is well described by[12]

$$E_{3_Q}(L) = 2\sigma L + c_Y - \frac{5}{2}\frac{\alpha_{3_Q}}{L}. \quad (2.27)$$

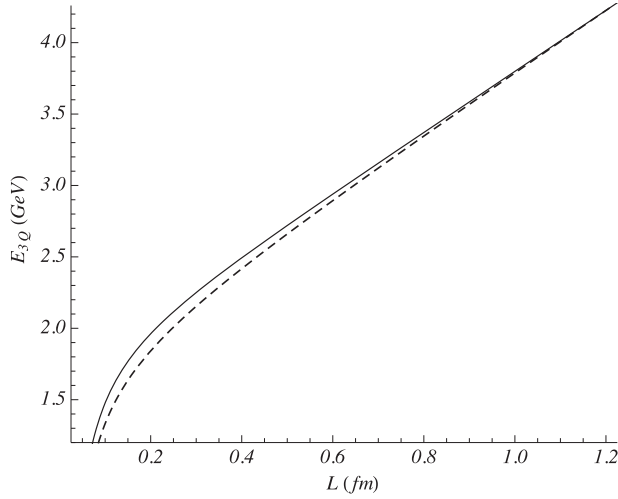[12]We set $c_Y = 1.71$ GeV to fit on the interval from 0.1 to 1.2 fm.

FIG. 5. The potential $E_{3_Q}(L)$ and Ansatz (2.27) (dashed) at $\mathfrak{g} = 0.176$, $s = 0.44$ GeV^2, $\kappa = -0.083$, $C = 1.87$ GeV, and $c_Y = 1.71$ GeV.

However, as seen from Fig. 5, this is not the case. The Ansatz (2.27) seems very good for short and long distances but not for intermediate ones. The picture is similar to that of Fig. 3, on the right. In other words, E_{3_Q} is a more complicated function of L than the function given by Eq. (2.27).

Let us make some estimates. In units of $\alpha_{Q\bar{Q}}$ and σ, we get

$$\frac{\alpha_{3_Q}}{\alpha_{Q\bar{Q}}} \approx 0.475, \qquad \frac{\sigma_0}{\sigma} \approx 0.926. \qquad (2.28)$$

The last ratio shows that there is a deviation from the Δ law defined by Eq. (1.1).

Looking again at Eq. (2.28) and back to Eq. (2.15), we see that the coefficients in the short distance expansion are not the same. It is a bit surprising but true that for the triangle geometry the coefficients are larger,[13]

$$\frac{\alpha_{3_Q}^c}{\alpha_{3_Q}^t} \approx 0.960, \qquad \frac{\sigma_0^c}{\sigma_0^t} \approx 0.920. \qquad (2.29)$$

Thus, these expansion coefficients are geometry dependent.

The long distance expansion is also puzzling. Although the physical string tension is universal (geometry independent), the constant terms are not. A simple estimate yields

$$c^c - c^t \approx 0.006 \text{ GeV}. \qquad (2.30)$$

Here, we have assumed that the normalization constants C are equal in both cases.

---

[13]We use the subscripts c and t to denote the following geometries: collinear and triangle.

This is one of the important aspects of the model. The first that comes to mind when thinking about a possible explanation for what we have found is that it has a stringy origin. The point may be that a string junction affects the shape of the three-quark potential not only at long but even at short distances. As a result, the coefficients in the short distance expansion become dependent of the geometry in question. This is another objection to the Δ law where $\alpha_{3_Q} = \frac{1}{2}\alpha_{Q\bar{Q}}$ for any geometry. Of course, it would be very interesting to see what this means for heavy baryon spectroscopy because neither the Δ nor Y law takes this effect into account.

D. Generic collinear geometry

With the experience we have gained, it is straightforward to generalize formulas such as Eqs. (2.19) and (2.20) and determine the three-quark potential for a generic case of collinear geometry.

Consider the symmetric configuration sketched in Fig. 4 on the left. To get further, we need to modify it by moving the first quark to a new position, say at $x_1 = -l$. Without loss of generality, we may move it closer to the origin such that $l \leq L$. The resulting configuration will be a deformation of the initial one, as shown in Fig. 4 on the right.

First, we will describe the gluing conditions, which is the easier thing to do. From Eq. (B12), we immediately obtain

$$\cos \alpha_1 - \cos \alpha_2 - \cos \alpha_3 = 0,$$
$$\sin \alpha_1 + \sin \alpha_2 + \sin \alpha_3 = 3\kappa(1 + 4\nu)e^{-3\nu}. \qquad (2.31)$$

Here, we have abbreviated α_{+i} to α_i.

Next, we should mention an important subtlety that arises when one tries to move Q_1 closer to Q_3. This subtlety is related to a flip of sign in α_1, the slope of the first string at the vertex. As a result, the shape of the first string changes from that of Fig. 10 on the right to that on the left. In the meantime, the other strings keep their shapes.

1. Configuration with $\alpha_1 < 0$

We will now make the discussion more concrete. Consider a small deformation of the symmetric configuration. In that case, we still have $\alpha_1 < 0$ and $\alpha_2 < 0$, but with $\alpha_3 \neq \frac{\pi}{2}$, as shown in Fig. 4 on the right.

If we consider the third string, then, in virtue of Eq. (A6), x_+ can be written as an integral. We will thus have

$$x_+ = -\cos\alpha_3 \sqrt{\frac{\nu}{\mathfrak{s}}} \int_0^1 dv_3 \, v_3^2 e^{\nu(1-v_3^2)} (1 - \cos^2\alpha_3 \, v_3^4 e^{2\nu(1-v_3^2)})^{-\frac{1}{2}}. \qquad (2.32)$$

Notice that x_+ is negative. The reason for this is a force balance at the vertex.

Similarly, for the first and second strings, $x_+ + l$ and $L - x_+$ can be expressed in terms of integrals by using Eq. (A16). Combining those with Eq. (2.32) leads one to

$$
l = \sqrt{\frac{\lambda_1}{\mathfrak{s}}} \left[\int_0^1 dv_1 v_1^2 e^{\lambda_1(1-v_1^2)} (1 - v_1^4 e^{2\lambda_1(1-v_1^2)})^{-\frac{1}{2}} \right.
$$
$$
+ \int_{\sqrt{\frac{\nu}{\lambda_1}}}^1 dv_1 v_1^2 e^{\lambda_1(1-v_1^2)} (1 - v_1^4 e^{2\lambda_1(1-v_1^2)})^{-\frac{1}{2}} \right]
$$
$$
+ \cos\alpha_3 \sqrt{\frac{\nu}{\mathfrak{s}}} \int_0^1 dv_3 v_3^2 e^{\nu(1-v_3^2)} (1 - \cos^2\alpha_3 v_3^4 e^{2\nu(1-v_3^2)})^{-\frac{1}{2}}
$$

$$(2.33)$$

and

$$
L = \sqrt{\frac{\lambda_2}{\mathfrak{s}}} \left[\int_0^1 dv_2 v_2^2 e^{\lambda_2(1-v_2^2)} (1 - v_2^4 e^{2\lambda_2(1-v_2^2)})^{-\frac{1}{2}} \right.
$$
$$
+ \int_{\sqrt{\frac{\nu}{\lambda_2}}}^1 dv_2 v_2^2 e^{\lambda_2(1-v_2^2)} (1 - v_2^4 e^{2\lambda_2(1-v_2^2)})^{-\frac{1}{2}} \right]
$$
$$
- \cos\alpha_3 \sqrt{\frac{\nu}{\mathfrak{s}}} \int_0^1 dv_3 v_3^2 e^{\nu(1-v_3^2)} (1 - \cos^2\alpha_3 v_3^4 e^{2\nu(1-v_3^2)})^{-\frac{1}{2}}.
$$

$$(2.34)$$

The energies of the first and second strings can be read from Eq. (A20), while that of the third can be read from Eq. (A9). Combining those with the expression (2.3) for the gravitational energy of the vertex, we find the total energy

$$
E_{3_Q} = \mathfrak{g} \sum_{i=1}^2 \sqrt{\frac{\mathfrak{s}}{\lambda_i}} \left[\int_0^1 \frac{dv_i}{v_i^2} (e^{\lambda_i v_i^2} (1 - v_i^4 e^{2\lambda_i(1-v_i^2)})^{-\frac{1}{2}} - 1 - v_i^2) \right.
$$
$$
+ \int_{\sqrt{\frac{\nu}{\lambda_i}}}^1 \frac{dv_i}{v_i^2} e^{\lambda_i v_i^2} (1 - v_i^4 e^{2\lambda_i(1-v_i^2)})^{-\frac{1}{2}} \right] + \mathfrak{g}\sqrt{\frac{\mathfrak{s}}{\nu}} \left[3\kappa e^{-2\nu} \right.
$$
$$
+ \int_0^1 \frac{dv_3}{v_3^2} (e^{\nu v_3^2} (1 - \cos^2\alpha_3 v_3^4 e^{2\nu(1-v_3^2)})^{-\frac{1}{2}} - 1 - v_3^2) \right]
$$
$$
+ C.
$$

$$(2.35)$$

First, let us see what happens if $\alpha_3 = \frac{\pi}{2}$. In this case, x_+ vanishes, and l becomes equal to L. In addition, the expression (2.35) reduces to that of Eq. (2.20). So, the above formulas are consistent with those of Sec. II. C.

Now, let us try to understand how the potential can be written parametrically as $E_{3_Q} = E(\lambda_1, \lambda_2)$, $l = l(\lambda_1, \lambda_2)$, and $L = L(\lambda_1, \lambda_2)$. It is easy to see from Eq. (A17) that

$$
\cos\alpha_i = \frac{\nu}{\lambda_i} e^{\lambda_i - \nu}, \qquad (2.36)
$$

with $i = 1, 2$. After a substitution into the first equation of Eq. (2.31), we find

$$
\cos\alpha_3 = \left(\frac{e^{\lambda_1}}{\lambda_1} - \frac{e^{\lambda_2}}{\lambda_2} \right) \nu e^{-\nu}. \qquad (2.37)
$$

From this, it follows that λ_1 and λ_2 must obey $\lambda_1 \leq \lambda_2$ if $\lambda_i \in [0, 1]$. Now, plugging Eqs. (2.36) and (2.37) into the second equation of Eq. (2.31), we obtain

$$
\left[1 - \frac{\nu^2}{\lambda_1^2} e^{2(\lambda_1 - \nu)} \right]^{\frac{1}{2}} + \left[1 - \frac{\nu^2}{\lambda_2^2} e^{2(\lambda_2 - \nu)} \right]^{\frac{1}{2}}
$$
$$
- \left[1 - \nu^2 e^{-2\nu} \left(\frac{e^{\lambda_2}}{\lambda_2} - \frac{e^{\lambda_1}}{\lambda_1} \right)^2 \right]^{\frac{1}{2}} + 3\kappa(1 + 4\nu)e^{-3\nu} = 0.
$$

$$(2.38)$$

Unfortunately, we do not know how to explicitly express one parameter as a function of two others. In practice, it is convenient to choose the λ's as independent parameters and then solve Eq. (2.38) for ν numerically.

To summarize, the three-quark potential is given in parametrical form by $E_{3_Q} = E(\lambda_1, \lambda_2)$, $l = l(\lambda_1, \lambda_2)$, and $L = L(\lambda_1, \lambda_2)$. The parameters take values on the interval [0, 1] and obey the inequality $\lambda_1 \leq \lambda_2$.

2. Configuration with $\alpha_1 = 0$

There is one important situation in which a transition between the two types of profile occurs. This is the case $\alpha_1 = 0$. Although the calculations are simple, it is useful for the purposes of the present paper to have explicit formulas.

A helpful observation which makes the analysis easy is the following. If $\alpha_1 = 0$, then $\nu = \lambda_1$, which follows from Eq. (2.36). Hence, there is only one independent parameter.

For $\lambda_1 = \nu$, Eqs. (2.33) and (2.34) take the form

$$
l = \sqrt{\frac{\nu}{\mathfrak{s}}} \left[\int_0^1 dv_1 v_1^2 e^{\nu(1-v_1^2)} (1 - v_1^4 e^{2\nu(1-v_1^2)})^{-\frac{1}{2}} \right.
$$
$$
+ \cos\alpha_3 \int_0^1 dv_3 v_3^2 e^{\nu(1-v_3^2)} (1 - \cos^2\alpha_3 v_3^4 e^{2\nu(1-v_3^2)})^{-\frac{1}{2}} \right]
$$

$$(2.39)$$

and

$$
L = \sqrt{\frac{\lambda_2}{\mathfrak{s}}} \left[\int_0^1 dv_2 v_2^2 e^{\lambda_2(1-v_2^2)} (1 - v_2^4 e^{2\lambda_2(1-v_2^2)})^{-\frac{1}{2}} \right.
$$
$$
+ \int_{\sqrt{\frac{\nu}{\lambda_2}}}^1 dv_2 v_2^2 e^{\lambda_2(1-v_2^2)} (1 - v_2^4 e^{2\lambda_2(1-v_2^2)})^{-\frac{1}{2}} \right]
$$
$$
- \cos\alpha_3 \sqrt{\frac{\nu}{\mathfrak{s}}} \int_0^1 dv_3 v_3^2 e^{\nu(1-v_3^2)}
$$
$$
\times (1 - \cos^2\alpha_3 v_3^4 e^{2\nu(1-v_3^2)})^{-\frac{1}{2}}.
$$

$$(2.40)$$

In the meantime, the expression for the total energy of the configuration becomes

$$E_{3_Q} = \mathfrak{g}\sqrt{\frac{\mathfrak{s}}{\nu}}\bigg[3\kappa e^{-2\nu} - 2$$

$$+ \int_0^1 \frac{dv_1}{v_1^2}(e^{\nu v_1^2}(1 - v_1^4 e^{2\nu(1-v_1^2)})^{-\frac{1}{2}} - 1)$$

$$+ \int_0^1 \frac{dv_3}{v_3^2}(e^{\nu v_3^2}(1 - \cos^2\alpha_3 v_3^4 e^{2\nu(1-v_3^2)})^{-\frac{1}{2}} - 1)\bigg]$$

$$+ \mathfrak{g}\sqrt{\frac{\mathfrak{s}}{\lambda_2}}\bigg[\int_0^1 \frac{dv_2}{v_2^2}(e^{\lambda_2 v_2^2}(1 - v_2^4 e^{2\lambda_2(1-v_2^2)})^{-\frac{1}{2}} - 1 - v_2^2)$$

$$+ \int_{\sqrt{\frac{\nu}{\lambda_2}}}^1 \frac{dv_2}{v_2^2} e^{\lambda_2 v_2^2}(1 - v_2^4 e^{2\lambda_2(1-v_2^2)})^{-\frac{1}{2}}\bigg] + C. \quad (2.41)$$

For completeness, we include the corresponding equations for $\cos\alpha_3$ and ν in our analysis. A short calculation shows that Eq. (2.37) becomes

$$\cos\alpha_3 = 1 - \frac{\nu}{\lambda_2}e^{\lambda_2-\nu} \quad (2.42)$$

and Eq. (2.38) becomes

$$\bigg[1 - \frac{\nu^2}{\lambda_2^2}e^{2(\lambda_2-\nu)}\bigg]^{\frac{1}{2}} - \bigg[1 - \bigg(1 - \frac{\nu}{\lambda_2}e^{\lambda_2-\nu}\bigg)^2\bigg]^{\frac{1}{2}}$$

$$+ 3\kappa(1 + 4\nu)e^{-3\nu} = 0. \quad (2.43)$$

Even for this simplified form, we do not know how to explicitly express ν as a function of λ_2, but of course it can be done numerically.

Now, let us see how the potential can be written parametrically as $E_{3_Q} = E(\nu, \lambda_2)$, $l = l(\nu, \lambda_2)$, and $L = L(\nu, \lambda_2)$. From Eqs. (A17) and (2.31), it follows that

$$\cos\alpha_1 = \cos\alpha_3 + \frac{\nu}{\lambda_2}e^{\lambda_2-\nu}. \quad (2.46)$$

Plugging this into the second equation of Eq. (2.31) gives

$$\bigg[1 - \frac{\nu^2}{\lambda_2^2}e^{2(\lambda_2-\nu)}\bigg]^{\frac{1}{2}} - \bigg[1 - \bigg(\cos\alpha_3 + \frac{\nu}{\lambda_2}e^{\lambda_2-\nu}\bigg)^2\bigg]^{\frac{1}{2}}$$

$$- [1 - \cos^2\alpha_3]^{\frac{1}{2}} + 3\kappa(1 + 4\nu)e^{-3\nu} = 0. \quad (2.47)$$

This equation can be used to solve, at least numerically, for $\cos\alpha_3$ under the given values of ν and λ_2.

Thus, in the case $\alpha_1 = 0$, the potential can be parametrically written as $E_{3_Q} = E(\lambda_2)$, $l = l(\lambda_2)$, and $L = L(\lambda_2)$. The parameter takes values on the interval [0, 1]. But one important fact about such a configuration is that it occurs only at specific values of l and L, as follows from the last two equations.

3. Configuration with $\alpha_1 > 0$

Finally, to complete the picture, we need to consider the configurations with $\alpha_1 > 0$. Such configurations exist for smaller l. This can be done by slightly extending what we have described so far. The novelty is that the first string has a shape similar to that of Fig. 10, on the left.

First, $x_+ + l$ is no longer expressed by Eq. (A16) but by Eq. (A6). Since the third string keeps its shape, Eq. (2.32) holds. From this, it follows that

$$l = \sqrt{\frac{\nu}{\mathfrak{s}}}\sum_{i=1,3}\int_0^1 dv_i v_i^2 e^{\nu(1-v_i^2)}\cos\alpha_i(1 - \cos^2\alpha_i v_i^4 e^{2\nu(1-v_i^2)})^{-\frac{1}{2}}.$$

$$(2.44)$$

At the same time, $L - x_+$ is expressed by Eq. (A16), which makes Eq. (2.34) true for $\alpha_1 > 0$ as well.

Second, the energy of the first string is now given by Eq. (A9) rather than by Eq. (A20). Making this replacement in Eq. (2.35), we get the total energy

$$E_{3_Q} = \mathfrak{g}\sqrt{\frac{\mathfrak{s}}{\lambda_2}}\bigg[\int_0^1 \frac{dv_2}{v_2^2}(e^{\lambda_2 v_2^2}(1 - v_2^4 e^{2\lambda_2(1-v_2^2)})^{-\frac{1}{2}} - 1 - v_2^2) + \int_{\sqrt{\frac{\nu}{\lambda_2}}}^1 \frac{dv_2}{v_2^2}e^{\lambda_2 v_2^2}(1 - v_2^4 e^{2\lambda_2(1-v_2^2)})^{-\frac{1}{2}}\bigg]$$

$$+ \mathfrak{g}\sqrt{\frac{\mathfrak{s}}{\nu}}\bigg[3\kappa e^{-2\nu} + \sum_{i=1,3}\int_0^1 \frac{dv_i}{v_i^2}(e^{\nu v_i^2}(1 - \cos^2\alpha_i v_i^4 e^{2\nu(1-v_i^2)})^{-\frac{1}{2}} - 1 - v_i^2)\bigg] + C. \quad (2.45)$$

At this point, it is worth noting that at $\alpha_1 = 0$ all the above formulas reduce to those of the previous section. This fact can be used as a self-consistency check of the results.

To summarize, the three-quark potential is given in parametric form by $E_{3_Q} = E(\nu, \lambda_2)$, $l = l(\nu, \lambda_2)$, and $L = L(\nu, \lambda_2)$. The parameters ν and λ_2 take values on the intervals $[0, \nu_0]$ and [0, 1], where ν_0 is a solution to Eq. (2.43) at $\lambda_2 = 1$.

4. What we have learned

In Fig. 6, we display our result for the potential $E_{3_Q}(l, L)$ obtained from the three different types of configurations. For simplicity, we restrict to the case $L \geq l$. Since the function E_{3_Q} is symmetric under the exchange of l and L, one can easily obtain E_{3_Q} for the opposite case by a reflection in the line $l = L$.
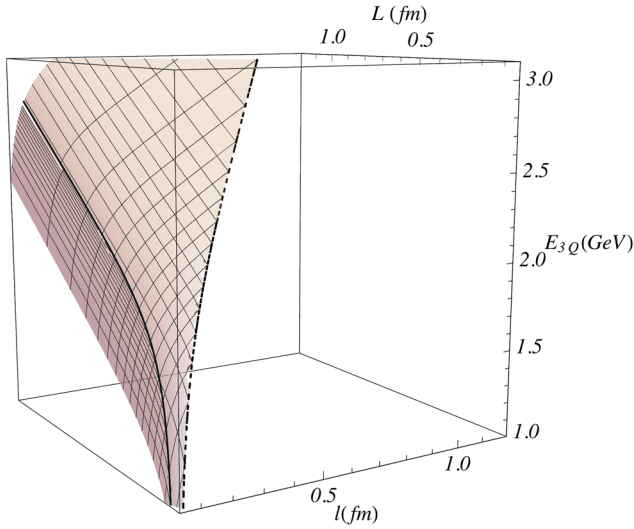
FIG. 6. The three-quark potential $E_{3_Q}(l, L)$ at $\mathfrak{g} = 0.176$, $s = 0.44 \text{ GeV}^2$, $\kappa = -0.083$, and $C = 1.87 \text{ GeV}$. The solid curve indicates where $\alpha_1 = 0$. The dashed curve represents the potential at $l = L$.

One lesson to learn from this example is that in the limit $\lambda_2 \to 1$, along the curve given by $\alpha_1 = 0$, the value of L goes to infinity, while that of l stays bounded. Indeed, it follows from Eq. (2.39) that $l(\lambda_2)$ is an increasing function of λ_2 of which the limiting value at $\lambda_2 = 1$ is given by

$$l_{\max} = \sqrt{\frac{\nu_0}{\mathfrak{s}}} \int_0^1 dv [(v^{-4} e^{2\nu_0(v^2-1)} - 1)^{-\frac{1}{2}}$$
$$+ ((1 - \nu_0 e^{1-\nu_0})^{-2} v^{-4} e^{2\nu_0(v^2-1)} - 1)^{-\frac{1}{2}}]. \quad (2.48)$$

The same conclusion is true for the configuration with $\alpha_1 > 0$. The separation l is bounded from above by $l_{\max}$, while L is not. This can also be seen from Fig. 6.

Let us make a simple estimate of $l_{\max}$. For the same parameter values as in Fig. 6, expression (2.48) yields $l_{\max} \approx 0.1$ fm. This value is compatible with an estimate for a size of the bb diquark obtained from $l \sim 2/m_b$.

Another lesson is that at large separations between the quarks, when both L and l go to infinity, the potential behaves like

$$E_{3_Q}(l, L) = \sigma(L + l) + c + o(1), \quad (2.49)$$

with c given by Eq. (2.26). To deduce this, we consider the configuration with $\alpha_1 < 0$ and use the fact that this limiting case corresponds to a small region near the point $(1, 1)$ in the parameter space (λ_1, λ_2). As in Sec. II. C, we expand the right-hand sides of Eqs. (2.33), (2.34), and (2.35) near $(1, 1)$ and then reduce the three equations to the single equation (2.49).

Besides looking for possible applications to phenomenology, it would be very interesting to confront our predictions with future numerical simulations.

III. MORE ON LIMITING CASES

In Sec. II, we took the collinear geometry as the basic example to illustrate the use of the string theory technique in practice. There is more to say if we consider the situation when two quarks get close to each other. In this case, a simplified treatment is to consider a system of two particles, the quark and diquark. The analysis of Sec. II allows us to shed some light on that situation.

A. Quark-diquark potential

It is known that in the limit of large quark masses QCD has a symmetry which relates hadrons with two heavy quarks to analogous states with one heavy antiquark [33]. This implies that we should be able to reproduce the heavy quark-antiquark potential from the results of Sec. II.

To show this, let us consider a collinear configuration with L fixed and $l \to 0$.[14] In this case, we should pick the configuration with $\alpha_1 > 0$. A short analysis shows that in terms of the parameters what we need is to take the limit $\nu \to 0$ with λ_2 fixed.

Letting $\nu \to 0$ in Eqs. (2.46) and (2.47), we get

$$\alpha_1 = \alpha_3, \quad \text{with} \quad \alpha_3 = \arcsin \frac{1 + 3\kappa}{2}. \quad (3.1)$$

These formulas mean that in this limit the angle α_2 becomes a right angle.

The result of taking $\nu \to 0$ in Eq. (2.44) is trivial, $l = 0$. But in Eq. (2.34), it turns out to be

$$L = 2\sqrt{\frac{\lambda_2}{\mathfrak{s}}} \int_0^1 dv_2 v_2^2 e^{\lambda_2(1-v_2^2)} (1 - v_2^4 e^{2\lambda_2(1-v_2^2)})^{-\frac{1}{2}}. \quad (3.2)$$

Notice that L is a continuously increasing function of λ_2. It vanishes at $\lambda_2 = 0$ and develops a logarithmic singularity at $\lambda_2 = 1$.

Taking the limit $\nu \to 0$ in Eq. (2.45) requires some care. Because of divergences at $\nu = 0$, we need a regulator that renders E_{3_Q} finite. The right procedure, which is consistent with what we did before, is to first replace ν by its lower bound. It is given by $\mathfrak{s}\epsilon^2$ as it follows from the lower bound on r. Then, the regularized expression for E_{3_Q} is given by

$$E_R = \mathfrak{g}\sqrt{\frac{\mathfrak{s}}{\lambda_2}} \left[\int_0^1 \frac{dv_2}{v_2^2} (e^{\lambda_2 v_2^2}(1 - v_2^4 e^{2\lambda_2(1-v_2^2)})^{-\frac{1}{2}} - 1 - v_2^2) \right.$$
$$+ \int_{\sqrt{\frac{\mathfrak{s}}{\lambda_2}\epsilon}}^1 \frac{dv_2}{v_2^2} e^{\lambda_2 v_2^2}(1 - v_2^4 e^{2\lambda_2(1-v_2^2)})^{-\frac{1}{2}} \right] + \frac{\mathfrak{g}}{\epsilon} \left[3\kappa e^{-2\mathfrak{s}\epsilon^2} \right.$$
$$+ 2\int_0^1 \frac{dv_1}{v_1^2} (e^{\mathfrak{s}\epsilon^2 v_1^2}(1 - \cos^2\alpha_1 v_1^4 e^{2\mathfrak{s}\epsilon^2(1-v_1^2)})^{-\frac{1}{2}}$$
$$\left. - 1 - v_1^2) \right] + C. \quad (3.3)$$

---

[14]One can think of l as a diquark size.

A little calculation reveals that the expansion in powers of ϵ takes the form

$$E_R = \frac{\mathfrak{g}}{\epsilon} E_0 + E_{\mathrm{QD}} + o(1), \qquad (3.4)$$

where E_0 is given by Eq. (C10). Notice that the singular term contains divergences coming from an infinitely large quark mass as well as self-energies of the vertex and strings. It is important that the coefficient E_0 does not depend on λ_2 and, as a consequence, on L. This allows one to deal with the divergence in a fashion similar to the standard treatment of power divergences in Wilson loops.

Subtracting the $\frac{1}{\epsilon}$ term and letting $\epsilon = 0$, we get a finite result,

$$E_{\mathrm{QD}} = 2\mathfrak{g}\sqrt{\frac{\mathfrak{s}}{\lambda_2}} \int_0^1 \frac{dv_2}{v_2^2} (e^{\lambda_2 v_2^2}(1 - v_2^4 e^{2\lambda_2(1-v_2^2)})^{-\frac{1}{2}}$$
$$- 1 - v_2^2) + C'. \qquad (3.5)$$

Here, C' is a normalization constant which is scheme dependent.

Equations (3.2) and (3.5) provide a parametric representation of the quark-diquark potential at distances much larger than the diquark size. This parametric representation coincides with that of Ref. [22] for the quark-antiquark potential, as expected [33].

B. Quark-quark potential

We will describe a static potential which represents a part of the interquark interaction inside heavy diquarks of small size. As above, we pick the configuration with $\alpha_1 > 0$. However, we now consider the case when l is small but nonzero and $L \to \infty$, as sketched in Fig. 7. This means that one quark is placed far away from the others such that its impact on the diquark can be easily assessed. From Eqs. (2.34) and (2.44), it follows that in terms of the parameters ν and λ_2 we need to consider a small region near the point $(0, 1)$ in the parameter space (ν, λ_2). The
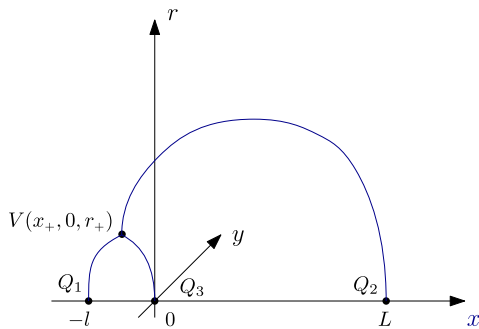

FIG. 7. A collinear configuration for $L \gg l$.

difference with what we have done in Sec. II. A is that in the expansions in powers of ν we should keep track of small terms which give rise to a term linear in l in the expression for the total energy.

With the help of the expansions (C8), one readily sees that for small l and large L the three-quark potential behaves like

$$E_{3_Q}(l,L) = -\frac{\alpha_{QQ}}{l} + \sigma_0 l + \sigma\left(L + \frac{1}{2}l\right) + \mathrm{c} + o(l), \quad (3.6)$$

where

$$\alpha_{QQ} = -l_0 E_0 \mathfrak{g},$$
$$\sigma_0 = \frac{1}{l_0}\left(E_1 + \frac{l_1}{l_0} E_0\right)\mathfrak{g}\mathfrak{s},$$
$$\mathrm{c} = 2\mathfrak{g}\sqrt{\mathfrak{s}} \int_0^1 \frac{dv}{v^2}(e^{v^2}(1 - v^4 e^{2(1-v^2)})^{\frac{1}{2}} - 1 - v^2) + C.$$
$$(3.7)$$

The l_i's and E_i's are given by Eqs. (C9) and (C10), respectively. Notice that in Eq. (3.7) the difference between c and C is written as an integral which is equal to that obtained in the quark-antiquark potential at long distances [26]. This is consistent with the symmetry [33].

There is an important subtlety that arises when one tries to extract the quark-quark potential from the above expression. This subtlety is related to the fifth dimension. The point is that in the limit we are considering the x coordinate of the vertex turns out to be $x_+ = -l/2$. In other words, the vertex is located between the Q_1 and Q_3 quarks, as shown in Fig. 7. In contrast, from the four-dimensional perspective, it should be located at $x_+ = 0$ because in the case of the collinear geometry the vertex (the Fermat point) coincides with Q_3.[15] Thus, we have to subtract from E_{3_Q} the term proportional to σ and a constant term. Such a constant term has to include a contribution from the integral on the right-hand side of the last equation in Eq. (3.7). These two terms represent the quark-diquark binding energy at large distances. As a result, we get

$$E_{QQ}(l) = -\frac{\alpha_{QQ}}{l} + \sigma_0 l + C' + o(l), \qquad (3.8)$$

with C' a normalization constant. This is the main result of this section.

Having derived the static quark-quark potential, we can make some estimates of α_{qq} and σ_0. Using the fitted value of κ, we get

---

[15]Note that in the model we are considering a projection of V on the boundary coincides with the Fermat point only in the infrared limit, when the quarks are far away from each other [17].

$$\frac{\alpha_{QQ}}{\alpha_{Q\bar{Q}}} \approx 0.466, \qquad \frac{\sigma_0}{\sigma} \approx 0.785. \qquad (3.9)$$

Here, we have used $\alpha_{Q\bar{Q}}$ from the quark-antiquark potential. Thus, our estimates suggest that the ratio $\alpha_{QQ}/\alpha_{Q\bar{Q}}$ is close to $\frac{1}{2}$ and that the effective string tension inside a heavy diquark is approximately 20% less than the physical tension.

In phenomenology,[16] the quark-quark potential is usually related to the quark-antiquark potential by Lipkin's rule. This is an Ansatz which says that $E_{QQ} = \frac{1}{2}E_{Q\bar{Q}}$ [35]. Our estimate of $\alpha_{QQ}/\alpha_{Q\bar{Q}}$ is relatively close to it, whereas that of σ_0/σ is somewhat larger.

It is also worth noting that in four dimensions a simple estimate based on a string model yields a larger value for the ratio σ_0/σ. It is $\frac{\sqrt{3}}{2} \approx 0.866$ [36]. The caution here is that the reason for decreasing the string tension is geometric and nothing similar happens once three quarks are placed on a straight line.

IV. EXAMPLE OF HYBRID THREE-QUARK POTENTIAL

Here, we will describe a special type of hybrid three-quark potentials, namely, the potentials of which the gluonic excitations are similar to those in the Σ_u^- potential for the quark-antiquark. For simplicity, we illustrate only the case in which one string is excited. The question we want to address is this: what is the impact of gluonic excitations on the physical picture we found for the ground state?

Consider the configuration of Fig. 2. We are going to modify it by exciting one string via gluonic excitations so that the quarks remain at the same positions, i.e., at the vertices of the equilateral triangle. Unfortunately, we know of no efficient way to describe all possible excitations [25,37] within our model. The only exception is the so-called Σ excitations which have zero angular momentum. From the five-dimensional point of view, such excitations may be modeled by cusps on the Nambu-Goto strings [26]. Importantly, cusps are allowed only in the radial direction that has no impact on smoothness of a four-dimensional picture.

One way to implement this is to insert a local object, called the defect, on a string [26]. Technically, it is quite similar to what we did before for the baryon vertex, with the only difference being that two strings join at a defect in the interior as shown in Fig. 11. By inserting the defect on the third string of Fig. 2, we construct a new configuration shown in Fig. 8. It is an example of a string picture (five-dimensional) of hybrid baryons. Notice that the configuration has a reflection symmetry with respect to the y axis.
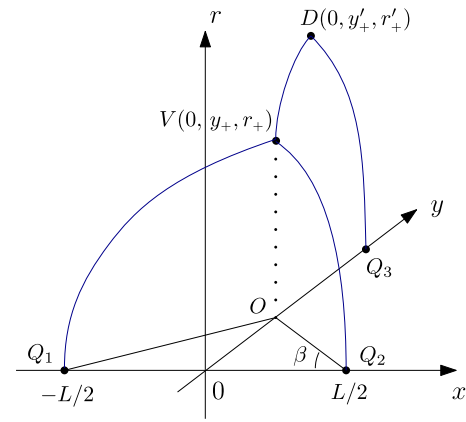

FIG. 8. A hybrid baryon configuration. The quarks Q_i are placed at the vertices of the equilateral triangle. V and D denote the vertex and defect.

Let us begin our analysis with the gluing conditions. As follows from the discussion in Appendix B, the only condition to be satisfied at the defect is that

$$\sin\alpha_3 - \kappa_d(1 + 4\lambda)e^{-3\lambda} = 0, \qquad (4.1)$$

with $\kappa_d = \frac{n}{2g}$. One can obtain it from Eq. (B7) by simply replacing ν with λ and α_1 with α_3. The conditions at the vertex are a bit more involved since there are two equations for force equilibrium, in the y and r directions. From Eq. (B14), it follows that

$$\cos\alpha_3' = 2\cos\alpha_1\sin\beta,$$
$$\sin\alpha_3' - 2\sin\alpha_1 + 3\kappa(1 + 4\nu)e^{-3\nu} = 0, \quad (4.2)$$

where β is the angle shown in Fig. 8. Notice that α_3' is positive and is related by Eq. (A15) to α_3 so that $\frac{e^\lambda}{\lambda}\cos\alpha_3 = \frac{e^\nu}{\nu}\cos\alpha_3'$.

In Sec. II, we observed that a string shape can change as a quark attached to its end point approaches another one. In the example we are analyzing, there is a similar story. A heuristic understanding of this can be obtained without resorting to explicit calculations, as follows. For large L, the configuration looks pretty much like that of Fig. 2 because a local defect has a little impact on very long strings. This implies that α_1 is negative. For small L, the strings become short, and we might expect the opposite to happen. It does happen when the defect has the dominant effect. In this case, shown in Fig. 8, the third string is stretched along the r axis from the boundary at $r = 0$ to a position of the defect at $r = r_+'$, whereas the vertex is located at $r = r_+$ such that $r_+ \ll r_+'$. It is obvious that α_1 is now positive. This means that a flip of sign in α_1 occurs at some value of L.

---

[16]See, e.g., Ref. [34] and references therein.

A. Configuration with $\alpha_1 < 0$

We begin with the case that the nonexcited strings have negative slopes at the vertex. Equation (A16) tells how to write the distance between the points Q_1 and O via an integral. It is

$$l_1 = \sqrt{\frac{\lambda_1}{\mathfrak{s}}} \left[\int_0^1 dv_1 v_1^2 e^{\lambda_1(1-v_1^2)}(1 - v_1^4 e^{2\lambda_1(1-v_1^2)})^{-\frac{1}{2}} \right. $$
$$\left. + \int_{\sqrt{\frac{\mu}{\lambda_1}}}^1 dv_1 v_1^2 e^{\lambda_1(1-v_1^2)}(1 - v_1^4 e^{2\lambda_1(1-v_1^2)})^{-\frac{1}{2}} \right], \qquad (4.3)$$

with $\frac{e^{\lambda_1}}{\lambda_1} = \frac{e^\nu}{\nu} \cos \alpha_1$.

Given Eqs. (A6) and (A11), we see that the distance between the point Q_3 and O can be represented as a sum of integrals

$$l_3 = \cos\alpha_3 \sqrt{\frac{\lambda}{\mathfrak{s}}} \left[\int_0^1 dv_3 v_3^2 e^{\lambda(1-v_3^2)}(1 - \cos^2\alpha_3 v_3^4 e^{2\lambda(1-v_3^2)})^{-\frac{1}{2}} \right.$$
$$\left. + \int_{\sqrt{\frac{\mu}{\lambda}}}^1 dv_3 v_3^2 e^{\lambda(1-v_3^2)}(1 - \cos^2\alpha_3 v_3^4 e^{2\lambda(1-v_3^2)})^{-\frac{1}{2}} \right]. \qquad (4.4)$$

Note that in order for the integrals to remain well defined and finite the condition must hold that $\lambda < \lambda_-$, where λ_- is a solution of equation $\cos\alpha_3 = \lambda e^{1-\lambda}$. In particular, in the limit $\lambda \to \lambda_-$, one has $l_3 \to \infty$. In this limit, l_1 also goes to infinity with ν going to ν_* which is defined by Eq. (2.9). For $\kappa_d = 1300$, the numerical calculation gives $\lambda_- \approx 3.29334$.

It is convenient to use the law of sines to complete the calculation for L. In the triangle OQ_1Q_3, we have

$$l_1 = \frac{L}{2\cos\beta} = \frac{l_3}{\sqrt{3}\cos\beta - \sin\beta}, \qquad (4.5)$$

which yields

$$L = l_1 \cos\beta. \qquad (4.6)$$

Coming back to the law of sines, we see that we must also satisfy the constraint

$$l_3 = l_1(\sqrt{3}\cos\beta - \sin\beta). \qquad (4.7)$$

The energies of the first and second strings can be read from Eq. (A20), while that of the third can be read from Eqs. (A9) and (A12). Combining those with Eqs. (2.3) and (2.4) for the gravitational energies of the vertex and defect, we find the total energy[17]

---

[17]We use a tilde to denote hybrid potentials.

$$\tilde{E}_{3_Q} = 2\mathfrak{g}\sqrt{\frac{\mathfrak{s}}{\lambda_1}} \left[\int_0^1 \frac{dv_1}{v_1^2} (e^{\lambda_1 v_1^2}(1 - v_1^4 e^{2\lambda_1(1-v_1^2)})^{-\frac{1}{2}} - 1 - v_1^2) \right.$$
$$\left. + \int_{\sqrt{\frac{\mu}{\lambda_1}}}^1 \frac{dv_1}{v_1^2} e^{\lambda_1 v_1^2}(1 - v_1^4 e^{2\lambda_1(1-v_1^2)})^{-\frac{1}{2}} \right]$$
$$+ \mathfrak{g}\sqrt{\frac{\mathfrak{s}}{\lambda}} \left[\int_0^1 \frac{dv_3}{v_3^2} \right.$$
$$\times (e^{\lambda v_3^2}(1 - \cos^2\alpha_3 v_3^4 e^{2\lambda(1-v_3^2)})^{-\frac{1}{2}} - 1 - v_3^2)$$
$$\left. + \int_{\sqrt{\frac{\mu}{\lambda}}}^1 \frac{dv_3}{v_3^2} e^{\lambda v_3^2}(1 - \cos^2\alpha_3 v_3^4 e^{2\lambda(1-v_3^2)})^{-\frac{1}{2}} \right]$$
$$+ 3\kappa\mathfrak{g}\sqrt{\frac{\mathfrak{s}}{\nu}}e^{-2\nu} + 2\kappa_d\mathfrak{g}\sqrt{\frac{\mathfrak{s}}{\lambda}}e^{-2\lambda} + C. \qquad (4.8)$$

Now, let us try to understand how the potential can be written parametrically as $\tilde{E}_{3_Q} = \tilde{E}(\lambda)$ and $L = L(\lambda)$. This is done in two steps. First, Eqs. (4.1) and (4.2) imply that the angles can be determined in terms of ν and λ. With this result, we have $\tilde{E}_{3_Q} = \tilde{E}(\lambda, \nu)$ and $L = L(\lambda, \nu)$. Finally, we use the constraint (4.7) to write ν in terms of λ. Unfortunately, we know of no ways to implement these steps analytically, but only numerically.

To summarize, the hybrid three-quark potential is given in parametrical form by $\tilde{E}_{3_Q} = \tilde{E}(\lambda)$ and $L = L(\lambda)$. The parameter takes values on the interval $[\lambda_0 0, \lambda_-]$, where $\lambda_0 0$ is defined below.

B. Configuration with $\alpha_1 = 0$

Now, we will discuss the case $\alpha_1 = 0$. As in the example of Sec. II, at $\alpha_1 = 0$, a transition between the two types of profiles occurs. Since there is only one parameter in the problem, the additional condition should be able to determine its value at the transition point, namely, $\lambda|_{\alpha_1=0} = \lambda_0 0$.

In this case, it is easy to explicitly show that

$$\sin\alpha_3' = -3\kappa(1 + 4\nu)e^{-3\nu},$$
$$\sin\beta = \frac{1}{2}[1 - 9\kappa^2(1 + 4\nu)^2 e^{-6\nu}]^{\frac{1}{2}} \qquad (4.9)$$

and, as a consequence, the relation between λ and ν is given by

$$\frac{e^\lambda}{\lambda}[1 - \kappa_d^2(1 + 4\lambda)^2 e^{-6\lambda}]^{\frac{1}{2}} = \frac{e^\nu}{\nu}[1 - 9\kappa^2(1 + 4\nu)^2 e^{-6\nu}]^{\frac{1}{2}}. \qquad (4.10)$$

The additional relation is provided by Eq. (4.7). Then, at least in principle, one can find ν and λ by solving the two equations simultaneously at given values of κ and κ_d. In practice, we can do it only numerically. For $\kappa = -0.083$

and $\kappa_d = 1300$, we get $\nu_0 \approx 0.99997$ and $\lambda_0 0 \approx 3.29326$. Importantly, we have found that $\lambda_0 0 < \lambda_-$, as expected for consistency. Finally, let us note that the value of L at the transition point turns out to be quite large. For the parameter values quoted above, it is about 2.83 fm.

C. Configuration with $\alpha_1 > 0$

Now, let us discuss the case $\alpha_1 > 0$. We can obtain the hybrid potential by making a simple modification to what we have described so far. The novelty here is that the shape of the nonexcited strings changes. This is important for understanding the short distance behavior of $\tilde{E}_{3_Q}$.

In this case, l_1 is expressed by Eq. (A6) and therefore takes the form

$$l_1 = \cos\alpha_1 \sqrt{\frac{\nu}{\mathfrak{s}}} \int_0^1 dv_1 v_1^2 e^{\nu(1-v_1^2)} (1 - \cos^2\alpha_1 v_1^4 e^{2\nu(1-v_1^2)})^{-\frac{1}{2}}.$$

(4.11)

In addition, the energies of the nonexcited strings are now expressed by Eq. (A9). Replacing the corresponding terms in Eq. (4.8), we obtain the total energy of the configuration:

$$\tilde{E}_{3_Q} = \mathfrak{g}\sqrt{\frac{\mathfrak{s}}{\nu}} \left[3\kappa e^{-2\nu} \right.$$
$$+ 2 \int_0^1 \frac{dv_1}{v_1^2} (e^{\nu v_1^2}(1 - \cos^2\alpha_1 v_1^4 e^{2\nu(1-v_1^2)})^{-\frac{1}{2}} - 1 - v_1^2) \right]$$
$$+ \mathfrak{g}\sqrt{\frac{\mathfrak{s}}{\lambda}} \left[2\kappa_d e^{-2\lambda} \right.$$
$$+ \int_0^1 \frac{dv_3}{v_3^2} (e^{\lambda v_3^2}(1 - \cos^2\alpha_3 v_3^4 e^{2\lambda(1-v_3^2)})^{-\frac{1}{2}} - 1 - v_3^2)$$
$$+ \int_{\sqrt{\frac{\nu}{\lambda}}}^1 \frac{dv_3}{v_3^2} e^{\lambda v_3^2}(1 - \cos^2\alpha_3 v_3^4 e^{2\lambda(1-v_3^2)})^{-\frac{1}{2}} \right] + C.$$

(4.12)

At this point, we can complete the parametric description of the three-quark potential. As before, the law of sines yields the expression for L and the constraint on the number of parameters. Thus, the hybrid three-quark potential is given by $\tilde{E}_{3_Q} = \tilde{E}(\lambda)$ and $L = L(\lambda)$, with the parameter taking values in the interval $[\lambda_+, \lambda_0 0]$. Here, λ_+ is a solution of equation $\sin\alpha_3 = 1$. Note that in the limit $\lambda \to \lambda_+$ one has $L \to 0$ and $\nu \to 0$. For $\kappa_d = 1300$, the numerical calculation gives $\lambda_+ \approx 3.27179$, which is consistent with $\lambda_+ < \lambda_0 0$.

D. What we have learned from this example

Having derived the expression for the hybrid three-quark potential, we can gain some understanding of what happens

to the physical picture we found for the ground state if gluonic excitations are of string nature.[18]

It is simplest to begin with the limiting cases: short and long distances L. To analyze the short distance behavior of $\tilde{E}_{3_Q}$, we consider the limit $\lambda \to \lambda_+$. First, we expand the right-hand sides of Eqs. (4.6) and (4.12) near $\lambda = \lambda_+$. Next, we reduce these equations to a single equivalent equation,

$$\tilde{E}_{3_Q}(L) = -\frac{\alpha_{QQ}}{L} + \tilde{C} + \sigma_0 L + \frac{3}{4}AL^2 + o(L^2), \quad (4.13)$$

where α_{QQ} and σ_0 are given by Eq. (3.7). In other words, the odd-term coefficients coincide with those of the quark-quark potential. The remaining even-term coefficients are

$$\tilde{C} = 2\mathfrak{g}\sqrt{\frac{\mathfrak{s}}{\lambda_+}}(\kappa_d e^{-2\lambda_+} - e^{\lambda_+} + \sqrt{\pi\lambda_+}\mathrm{Erfi}(\sqrt{\lambda_+})) + C,$$

$$A = \mathfrak{g}\mathfrak{s}^{\frac{3}{2}}(\sqrt{\pi}\mathrm{Erf}(\sqrt{\lambda_+}) - 2\sqrt{\lambda_+}e^{-\lambda_+})^{-1}. \quad (4.14)$$

These coincide with those of the Σ_u^- hybrid potential [26].[19] Note that the factor $\frac{3}{4}$ is of geometric nature. The excited string is perpendicular to the side of the triangle such that the distance between its end points is equal to the height of the triangle $h = \frac{\sqrt{3}}{2}L$.

Equation (4.13) has some conceptual interest. Let us first write it as

$$\tilde{E}_{3_Q}(L) = E_{QQ}(L) + \tilde{E}_{Q\bar{Q}}(h) + o(L^2). \quad (4.15)$$

This formula shows that at short distances the hybrid three-quark potential is described by a sum of two-body potentials. Using Eqs. (3.8) and (3.9) and keeping only the leading terms, we obtain

$$\tilde{E}_{3_Q}(L) \approx \frac{1}{2}E_{Q\bar{Q}}(L) + \tilde{E}_{Q\bar{Q}}(L). \quad (4.16)$$

This result is notable because it suggests a relation between the hybrid three-quark and quark-antiquark potentials. In Appendix D, we give a more detailed and precise account of this relation, which is in fact a generalization of the Δ law.

Another interesting conclusion one can draw from Eq. (4.13) is that it suggests that the quark-quark potential (3.8), which is defined when one starts with E_{3_Q} and then takes one quark away from the others, is universal (geometry independent).[20]

---

[18]Alternatively, there may be an option of getting hybrid potentials by exciting the baryon vertex.

[19]For the constant term, it only makes sense to speak of the scheme-independent part $\tilde{C} - C$.

[20]This issue was raised by Ph. de Forcrand. In an effort to provide more evidence, we have carried out the calculation using the same geometry as that of Ref. [36]. See Appendix E for more details.
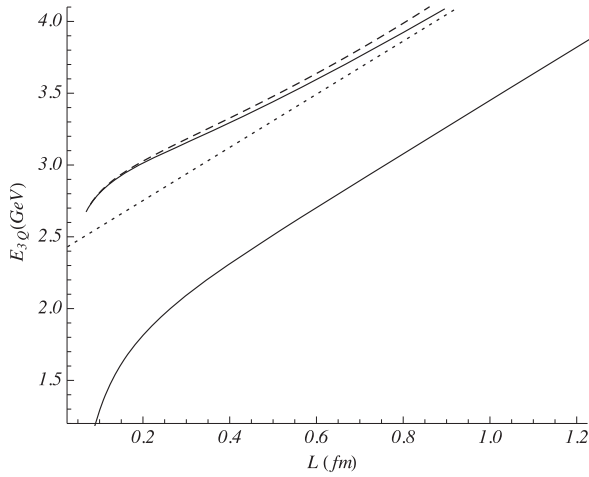
FIG. 9. The static three-quark potential and its hybrid excitation obtained on an equilateral triangle of side length L. The dashed curve corresponds to the Δ law (4.13), and the dotted one corresponds to the Y law (4.17).

In a similar spirit, we can explore the long distance behavior of $\tilde{E}_{3_Q}$. Expanding now the right-hand sides near $\lambda = \lambda_-$, we reduce the two equations to a single one:

$$\tilde{E}_{3_Q}(L) = \sqrt{3}\sigma L + c + \Delta + o(1). \qquad (4.17)$$

Here, c is the same constant as that in the expression (2.13) for the ground state.

The basic fact about Eqs. (2.12) and (4.17) is a finite gap between $\tilde{E}_{3_Q}$ and E_{3_Q} at large L. Explicitly, it is given by

$$\Delta = \lim_{L \to \infty} \tilde{E}_{3_Q}(L) - E_{3_Q}(L)$$
$$= 2\mathfrak{g}\sqrt{\mathfrak{s}} \left[\frac{\kappa_d}{\sqrt{\lambda_-}} e^{-2\lambda_-} + \int_1^{\sqrt{\lambda_-}} \frac{dv}{v^2} e^{v^2} (1 - v^4 e^{2(1-v^2)})^{\frac{1}{2}} \right].$$
$$(4.18)$$

The result agrees with the calculation of Ref. [26] for the hybrid quark-antiquark potentials. This suggests that the gap Δ, like the physical string tension σ, is universal (geometry independent). It is one of the main results of this paper.

Now a question arises: what happens in between? In Fig. 9, we display our results for the three-quark potentials.

Here, in addition to the parameters of Fig. 3, there is the parameter κ_d. We set $\kappa_d = 1300$ by fitting the gap to $\Delta = 0.78$ GeV.[21] Notice that it deviates from the value $\kappa_d = 2000$ used in Ref. [26]. This might seem strange, but it is easily explained. The point is that A is a slow varying

function of κ_d. Indeed, a numerical calculation shows that $A(2000)/A(1300) \approx 0.99$. This is the reason for the deviation if κ_d is fitted to A.

For large L, our model reveals the Y law, as it follows from the slope in Eq. (4.17). In contrast, the Δ law (4.13) yields the smaller slope equal to that of Sec. II. It is worth noting that $\tilde{E}_{3_Q}$ approaches the linear behavior at larger separations than E_{3_Q} does. The linear approximation is accurate enough for $\tilde{E}_{3_Q}$ when $L \geq 1$ fm compared to $L \geq 0.6$ fm for E_{3_Q} [18]. For small L, the Δ law is a good approximation to $\tilde{E}_{3_Q}$. However, the deviation increases with L, as seen from Fig. 9. Thus, our model predicts that for hybrid potentials the physical picture remains essentially the same: it incorporates two-body interactions at short distances and a genuine three-body interaction at longer ones.

We conclude our discussion of this example by making a couple of remarks. First, one can see from Fig. 9 that the function $\tilde{E}_{3_Q}(L)$ has an inflection point at $L = L_i$. The expression (4.13) allows one to make an estimate of L_i. It is $L_i \approx 0.34$ fm. Interestingly, in Eq. (4.13), the $1/L$ and L^2 terms cancel each other at $L = L_i$. Second, we have considered the case when only one string is excited. The generalization to the case in which two or three strings are excited is straightforward, but technical and more elaborate.

V. CONCLUDING COMMENTS

The purpose of this paper has been to make predictions based on the success of previous work [18,22,26]. The motivation was to gain some understanding of how baryons are put together from quarks.

The model we are pursuing has led to a number of interesting conclusions:

(1) The usual view on the three-quark potential is that the potential can be well approximated by the Δ law (1.1) at short distances and by the Y law (1.2) at long ones.[22] Mathematically, the point is that it is described by a complicated function of which the asymptotic behavior is given by those laws. We found that a further refinement of this view should take into account that in Eqs. (1.1) and (1.2) the coefficients α_{3_Q} and c are not universal but dependent of a geometry of sources (quarks). Translating into mathematical language, the coefficients depend on angular variables. Physically, this is a signature of genuine three-body interactions, even at short distances.

(2) The given example of a hybrid three-quark potential suggests that one may regard the Δ and Y laws as

---

[21]This value was determined from the spectra of closed string excitations [38]. It is quite close to that determined from the hybrid potentials [25,26]. This fact also suggests the universality of the gap.

[22]Interestingly, a similar pattern also occurs in three dimensions [39]. Here, it was found that a Lüscher-like correction, which is subleading to a constant term in the long-distance expansion of the three-quark potential, is geometry dependent [40].

good approximations to the hybrid potentials as well.

(3) There are at least two possible ways to cross check our findings. One way is by performing lattice simulations, and another is by multiloop calculations in perturbative QCD [41].

(4) The model we are developing is an effective string theory based on the Nambu-Goto formalism in a curved space. Therefore, it has some limitations. In particular, an issue of the Lüscher-like correction remains unclear. Another unclear issue is that a force of attraction occurs between the vertex and the boundary. What could be the reason for this? m is a result of a resummation of infinitely many terms (α' corrections) in the 5-brane action. Is it negative because the brane tension is negative, and if so, does it lead to instability?[23] These questions have no obvious answers. The Green-Schwarz formalism, already developed for strings on AdS$_5 \times$ S^5 [43], seems more appropriate to address these issues. However, this is still far from having been implemented. It is even not clear whether the Ansatz (2.2), which is a deformation of AdS$_5 \times$ S^5, is a solution of the supergravity equations. If so, what role do the other background fields play in QCD? What is clear is that finding the way to the string description of QCD is a challenging and difficult problem, and along the way, we will see and experience a lot of things [44]. In the meantime, lattice gauge theory and effective string models will remain the main tools of investigation.

ACKNOWLEDGMENTS

APPENDIX A: STATIC NAMBU-GOTO STRING WITH FIXED END POINTS

In this Appendix, we will discuss a static Nambu-Goto string in the curved geometry (2.2). The results provide the grounds for building multistring configurations.

---

[23]This is not so obvious because a baryonic configuration is not a single brane but a bound state, and the value we need is quite small. There has been an extensive discussion of negative tension branes, but in other contexts [42].

The Nambu-Goto action is given by

$$S = \frac{1}{2\pi\alpha'} \int_0^1 d\sigma \int_0^T d\tau \sqrt{\gamma}, \tag{A1}$$

with γ an induced metric on the string world sheet (with Euclidean signature). Consider a string stretched between the two fixed points $P(x_-, r_-)$ and $B(x_+, r_+)$ in the xr plane such that $x_+ \geq x_-$ and $r_+ \geq r_-$. This implies the following boundary conditions:

$$x(0) = x_-, \quad x(1) = x_+, \quad r(0) = r_-, \quad r(1) = r_+. \tag{A2}$$

In the static gauge, $t = \tau$ and $x = a\sigma + b$, the action takes the form

$$S = T\mathfrak{g} \int_{x_-}^{x_+} dx w(r) \sqrt{1 + (\partial_x r)^2}, \quad \text{with} \quad w(r) = \frac{e^{\mathfrak{g}r^2}}{r^2}. \tag{A3}$$

For convenience, we use the shorthand notation $\mathfrak{g} = \frac{R^2}{2\pi\alpha'}$ and $\partial_x r = \frac{\partial r}{\partial x}$. Since the integrand in Eq. (A3) does not depend explicitly on x, the Euler-Lagrange equation has the first integral

$$I = \frac{w(r)}{\sqrt{1 + (\partial_x r)^2}}. \tag{A4}$$

At the end points, I can be written as

$$I = w(r_\pm) \cos\alpha_\pm, \tag{A5}$$

where $\tan\alpha_\pm = \partial_x r|_{x=x_\pm}$ and $\alpha_\pm \in [-\frac{\pi}{2}, \frac{\pi}{2}]$.

In general, α_+ can be positive or negative. If $\alpha_+ > 0$, then a function $r(x)$ describing a string profile is increasing on the interval $[x_-, x_+]$. If $\alpha_+ < 0$, then the situation is a little bit more complicated. $r(x)$ is increasing on the interval $[x_-, x_{max}]$ and decreasing on the interval $[x_{max}, x_+]$ such that it has a maximum at $x = x_{max}$. Examples for both cases are sketched in Fig. 10. First, we describe the case of positive α_+.

1. Case $\alpha_+ \geq 0$

We begin with the case in which P lies on the boundary, which means $= 0$. After expressing I in terms of α_+ and r_+, we get a differential equation $w(r_+)\cos\alpha_+ = w(r)/\sqrt{1 + (\partial_x r)^2}$ that can be integrated over the variables x and r. So, we have
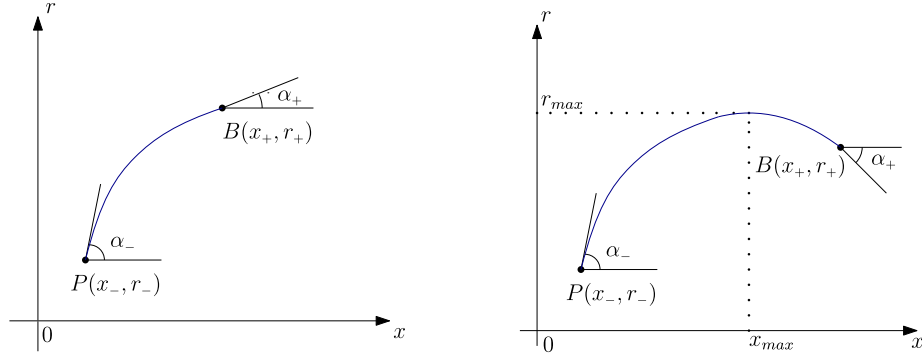
FIG. 10. A string stretched between two points. $\alpha_\pm$ denote the tangent angles at these points. We assume that $r_+ < 1/\sqrt{\mathsf{s}}$. Left: The case $\alpha_+ > 0$. Right: The case $\alpha_+ < 0$.

$$\ell = x_+ - x_- = \cos\alpha_+ \sqrt{\frac{\nu_+}{\mathsf{s}}} \int_0^1 dv\, v^2 e^{\nu_+(1-v^2)}$$
$$\times (1 - \cos^2\alpha_+ v^4 e^{2\nu_+(1-v^2)})^{-\frac{1}{2}}, \qquad (A6)$$

where $\nu_\pm = \mathsf{s} r_\pm^2$. This integral is well defined for $\nu_+ < 1$, while for larger values of ν_+, it becomes ill defined unless $\nu_+ e^{1-\nu_+} \geq \cos\alpha_+$.

Having derived the expression for the string length along the x axis, we can give a formal recipe for computing the energy of the string. First, we reduce the integral over x in S to that over r. This is easily done by using the first integral. Since the integral is divergent at $r = 0$, we regularize it by imposing a cutoff ϵ such that $r \geq \epsilon$. Finally, the regularized expression is given by

$$E_R = \frac{S_R}{T} = \mathsf{g}\sqrt{\frac{\mathsf{s}}{\nu_+}} \int_{\sqrt{\frac{\mathsf{s}}{\nu_+}}\epsilon}^1 \frac{dv}{v^2} e^{\nu_+ v^2} (1 - \cos^2\alpha_+ v^4 e^{2\nu_+(1-v^2)})^{-\frac{1}{2}}.$$
$$(A7)$$

In the limit as $\epsilon \to 0$, it behaves like

$$E_R = \frac{\mathsf{g}}{\epsilon} + E + O(\epsilon). \qquad (A8)$$

Subtracting the $\frac{1}{\epsilon}$ term and letting $\epsilon = 0$, we get a finite result,

$$E = \mathsf{g}\sqrt{\frac{\mathsf{s}}{\nu_+}} \int_0^1 \frac{dv}{v^2} \left(e^{\nu_+ v^2} (1 - \cos^2\alpha_+ v^4 e^{2\nu_+(1-v^2)})^{-\frac{1}{2}} \right.$$
$$\left. - 1 - v^2 \right) + c, \qquad (A9)$$

with c a normalization constant.

If we set $\alpha_+ = \frac{\pi}{2}$, then the string becomes straight. In that case, we obtain

$$\ell = 0, \qquad E = \mathsf{g}\sqrt{\frac{\mathsf{s}}{\nu_+}} \left(\sqrt{\pi\nu_+}\text{Erfi}(\sqrt{\nu_+}) - e^{\nu_+} \right) + c,$$
$$(A10)$$

which is the form in which it is written in Ref. [45]. $\text{Erfi}(x)$ is the imaginary error function.

It is straightforward to extend this analysis to the case in which the end point P is not on the boundary but in the interior such that $r_- > \epsilon$. As before, we express I in terms of α_+ and r_+ and then integrate the differential equation. After doing so, we find

$$\ell = \cos\alpha_+ \sqrt{\frac{\nu_+}{\mathsf{s}}} \int_{\sqrt{\frac{\nu_-}{\nu_+}}}^1 dv\, v^2 e^{\nu_+(1-v^2)}$$
$$\times (1 - \cos^2\alpha_+ v^4 e^{2\nu_+(1-v^2)})^{-\frac{1}{2}}. \qquad (A11)$$

The integral is well defined for $\nu_\pm > 1$. It becomes ill defined for smaller values unless $\cos\alpha_+ \leq \nu_+ e^{1-\nu_+}$ for $\nu_- < 1$ and $\cos\alpha_+ \leq \frac{\nu_+}{\nu_-} e^{\nu_- - \nu_+}$ for $\nu_\pm < 1$.

Then, we compute the energy

$$E = \mathsf{g}\sqrt{\frac{\mathsf{s}}{\nu_+}} \int_{\sqrt{\frac{\nu_-}{\nu_+}}}^1 \frac{dv}{v^2} e^{\nu_+ v^2} (1 - \cos^2\alpha_+ v^4 e^{2\nu_+(1-v^2)})^{-\frac{1}{2}}.$$
$$(A12)$$

In that case, there is no need for regularization.

We could of course have defined the first integral in terms of α_- and r_-. This gives an equivalent result,

$$\ell = \cos\alpha_- \sqrt{\frac{\nu_-}{\mathsf{s}}} \int_1^{\sqrt{\frac{\nu_+}{\nu_-}}} dv\, v^2 e^{\nu_-(1-v^2)}$$
$$\times (1 - \cos^2\alpha_- v^4 e^{2\nu_-(1-v^2)})^{-\frac{1}{2}}, \qquad (A13)$$

$$E = \mathsf{g}\sqrt{\frac{\mathsf{s}}{\nu_-}} \int_1^{\sqrt{\frac{\nu_+}{\nu_-}}} \frac{dv}{v^2} e^{\nu_- v^2} (1 - \cos^2\alpha_- v^4 e^{2\nu_-(1-v^2)})^{-\frac{1}{2}}.$$
$$(A14)$$

It is easy to see that a rescaling $v \to \sqrt{\frac{\nu_+}{\nu_-}} v$ reduces these expressions to those in Eqs. (A11) and (A12). Another useful formula is

$$\cos \alpha_- \frac{e^{\nu_-}}{\nu_-} = \cos \alpha_+ \frac{e^{\nu_+}}{\nu_+}, \qquad (A15)$$

which follows from Eq. (A5).

2. Case $\alpha_+ \leq 0$

What we have done so far generalizes straightforwardly to the case $\alpha_+ \leq 0$. An important point, which applies to all expressions written below, is that there are two contributions: one comes from the interval $[x_-, x_{\max}]$ on which $r(x)$ is increasing and the other from the interval $[x_{\max}, x_+]$ on which $r(x)$ is decreasing (see Fig. 10). Since the case $r_- \neq 0$ is not so important for our applications, we put the string end point P on the boundary.

If we define the first integral at $r = r_{\max}$ such that $I = w(r_{\max})$ and then integrate the differential equation (A4) over both intervals, we get

$$\ell = \sqrt{\frac{\lambda}{\mathfrak{s}}} \left[\int_0^1 dv \, v^2 e^{\lambda(1-v^2)} (1 - v^4 e^{2\lambda(1-v^2)})^{-\frac{1}{2}} \right.$$
$$\left. + \int_{\sqrt{\frac{\nu_+}{\lambda}}}^1 dv \, v^2 e^{\lambda(1-v^2)} (1 - v^4 e^{2\lambda(1-v^2)})^{-\frac{1}{2}} \right], \qquad (A16)$$

with $\lambda = \mathfrak{s} r_{\max}^2$ and $\nu_+ < \lambda$. The integrals are well defined if λ takes values in the interval $[0, 1]$.

The alternative to what we have done is to directly use Eqs. (A6) and (A11). The first term is obtained by setting $\alpha_+ = 0$ in Eq. (A6) and then replacing ν_+ by λ. By combining this with $\nu_- \to \nu_+$ in Eq. (A11), one reaches the desired result.

It is worth noting that λ, ν_+, and α_+ are not independent. From Eq. (A4), it follows that

$$\frac{e^\lambda}{\lambda} = \frac{e^{\nu_+}}{\nu_+} \cos \alpha_+. \qquad (A17)$$

Moreover, λ, as a function of ν_+ and α_+, can be written in terms of the ProductLog function as

$$\lambda = -\text{ProductLog}(-\nu_+ e^{-\nu_+}/\cos \alpha_+), \qquad (A18)$$

where $\text{ProductLog}(z)$ is the principal solution for w in $z = w e^w$ [31].

As in our previous case, the energy of the string can computed by first replacing the integral over x in S to that over r and then imposing the short distance cutoff on r. A calculation along the above lines gives

$$E_R = \mathfrak{g} \sqrt{\frac{\mathfrak{s}}{\lambda}} \left[\int_{\sqrt{\frac{\mathfrak{s}}{\lambda}\epsilon}}^1 \frac{dv}{v^2} e^{\lambda v^2} (1 - v^4 e^{2\lambda(1-v^2)})^{-\frac{1}{2}} \right.$$
$$\left. + \int_{\sqrt{\frac{\nu_+}{\lambda}}}^1 \frac{dv}{v^2} e^{\lambda v^2} (1 - v^4 e^{2\lambda(1-v^2)})^{-\frac{1}{2}} \right]. \qquad (A19)$$

To obtain from E_R a finite result, we need to subtract the $\frac{1}{\epsilon}$ term and then let $\epsilon = 0$. Finally, we are left with

$$E = \mathfrak{g} \sqrt{\frac{\mathfrak{s}}{\lambda}} \left[\int_0^1 \frac{dv}{v^2} \left(e^{\lambda v^2} (1 - v^4 e^{2\lambda(1-v^2)})^{-\frac{1}{2}} - 1 - v^2 \right) \right.$$
$$\left. + \int_{\sqrt{\frac{\nu_+}{\lambda}}}^1 \frac{dv}{v^2} e^{\lambda v^2} (1 - v^4 e^{2\lambda(1-v^2)})^{-\frac{1}{2}} \right] + c, \qquad (A20)$$

where c is the normalization constant. By essentially the same arguments that we have given for ℓ, the expression for E can be obtained directly from Eqs. (A9) and (A12).

We conclude this discussion with a couple of remarks. First of all, in the case $\alpha_+ = 0$, the expressions (A16) and (A20) are equal to those obtained in the previous section. Clearly, in this situation, the string profiles sketched in Fig. 10 coincide with each other.

Although the case $\alpha_+ = \frac{\pi}{2}$ is trivial, we have presented it above for completeness reasons; the case $\alpha_+ = -\frac{\pi}{2}$ needs a special care. The key point is that the string end point B approaches the boundary as $\alpha_+ \to -\frac{\pi}{2}$. Clearly, if I is finite, then $w(r_+)$ has to be infinite. This means that ν_+ goes to zero as α_+ goes to $-\frac{\pi}{2}$. There is no difficulty with Eq. (A16) because both integrals are convergent. Thus, we have

$$\ell = 2\sqrt{\frac{\lambda}{\mathfrak{s}}} \int_0^1 dv \, v^2 e^{\lambda(1-v^2)} (1 - v^4 e^{2\lambda(1-v^2)})^{-\frac{1}{2}}. \qquad (A21)$$

However, in Eq. (A20) the second integral becomes divergent at $v = 0$. We cut off the integral by placing a lower bound $\sqrt{\frac{\mathfrak{s}}{\lambda}}\epsilon$. This is consistent with what we did before. Indeed, a lower bound $r \geq \epsilon$ implies a lower bound for ν_+ of the form $\nu_+ \geq \mathfrak{s}\epsilon^2$. As a result, the regularized expression is simply

$$E_R = \mathfrak{g} \sqrt{\frac{\mathfrak{s}}{\lambda}} \left[\int_0^1 \frac{dv}{v^2} \left(e^{\lambda v^2} (1 - v^4 e^{2\lambda(1-v^2)})^{-\frac{1}{2}} - 1 - v^2 \right) \right.$$
$$\left. + \int_{\sqrt{\frac{\mathfrak{s}}{\lambda}\epsilon}}^1 \frac{dv}{v^2} e^{\lambda v^2} (1 - v^4 e^{2\lambda(1-v^2)})^{-\frac{1}{2}} \right] + c. \qquad (A22)$$

It diverges for $\epsilon \to 0$ as $\frac{\mathfrak{g}}{\epsilon}$. After subtracting the divergence, we get a finite result,

$$E = 2\mathfrak{g} \sqrt{\frac{\mathfrak{s}}{\lambda}} \int_0^1 \frac{dv}{v^2} \left(e^{\lambda v^2} (1 - v^4 e^{2\lambda(1-v^2)})^{-\frac{1}{2}} - 1 - v^2 \right) + 2c. \qquad (A23)$$
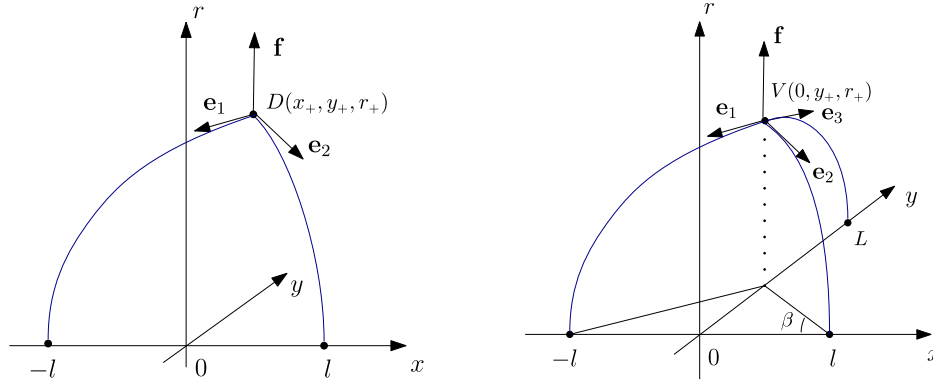
FIG. 11. String meeting at junctions. The gravitational force acting on junctions is directed in the upward vertical direction. Left: Two strings meeting at a defect placed at D. Right: Three strings meeting at a baryon vertex placed at V.

Here, λ is a parameter taking values in [0, 1]. The normalization constant is equal to $2c$ because of the double subtraction of $\frac{1}{\epsilon}$. Note that the expressions (A21) and (A23) coincide with those obtained in Ref. [22] for a string stretched between points on the boundary, as expected.

APPENDIX B: GLUING CONDITIONS

The string solutions discussed in Appendix A provide the basic blocks for building multistring configurations. What is also needed are certain gluing conditions for such blocks. The goal here is to describe those conditions.

From the physical viewpoint, the gluing conditions arise as follows. Strings meet at common junctions such as baryon vertices or defects. Clearly, a static baryon configuration must obey the condition that a net force vanishes at any junction. It is straightforward to translate this into a mathematical language. Extremizing the total action of a system of Nambu-Goto strings and junctions with respect to a location of the i junction, one gets a force balance condition at that location.[24] To illustrate how this works in practice, we follow Refs. [17,26] and consider two basic examples: two strings meeting at a defect and three strings meeting at a baryon vertex.

1. Two strings meeting at a defect

It is simplest to begin with two strings meeting at a defect. Such a defect results in a cusp formation in the $r_- =$ direction that represents a kind of string excitation [26].

We take two Nambu-Goto strings beginning at the heavy quark sources on the boundary and ending on the defect in the interior, as shown in Fig. 11 on the left. In this case, the total action of the configuration reads

$$S = \sum_{i=1}^{2} S_i + S_{\text{def}}, \qquad (B1)$$

where S_i is the action of the i string and S_{def} is that of the defect. It is given by Eq. (2.4).

Since we are interested in a static configuration, it is convenient to choose gauge conditions

$$t_i(\tau_i) = \tau_i, \qquad x_i(\sigma_i) = a_i \sigma_i + b_i, \qquad (B2)$$

with (τ_i, σ_i) the world sheet coordinates. Then the action of the i string takes the form

$$S_i = T\mathfrak{g} \int_0^1 d\sigma_i w \sqrt{a_i^2 + y_i'^2 + r_i'^2}, \qquad (B3)$$

where a prime denotes a derivative with respect to σ_i.

For the configuration shown in Fig. 11, the boundary conditions on the fields are given by

$$x_i(0) = \mp \ell, \qquad x_i(1) = x_+, \qquad y_i(0) = 0,$$
$$y_i(1) = y_+, \qquad r_i(0) = 0, \qquad r_i(1) = r_+. \qquad (B4)$$

Using these conditions, one can find the coefficients a_i and b_i. The result is $a_i = x_+ \pm \ell$ and $b_i = \mp \ell$.

A useful observation is that the Euler-Lagrange equations derived from S_i have the first integrals

$$I_i = \frac{w_i}{\sqrt{a_i^2 + y_i'^2 + r_i'^2}}, \qquad P_i = y_i', \qquad (B5)$$

which allows one to determine the y_i's. From Eq. (B4), it follows that $y_i(\sigma_i) = y_+ \sigma_i$.

It is now straightforward to extremize the total action with respect to the location of the defect. A short calculation gives

$$a_1 I_1 + a_2 I_2 = 0, \qquad (I_1 + I_2) y_+ = 0,$$
$$r_1'(1) I_1 + r_2'(1) I_2 + \mathfrak{g}^{-1} \partial_{r_+} \mathcal{V}(r_+) = 0, \qquad (B6)$$

with $\mathcal{V}(r) = n\frac{e^{-2\mathfrak{s}r^2}}{r}$, as follows from Eq. (2.4). We have defined the I_i's at $\sigma_i = 1$.

From the second equation, it follows that $y_+ = 0$. In other words, the static configuration lies in the xr plane. In that case, the first equation reduces to $\cos\alpha_{+1} = \cos\alpha_{+2}$, with α_{+i} the tangent angles at D. Its solution is simply $\alpha_{+1} = \alpha_{+2}$.[25] Of course, all of this may be understood using the symmetry analysis alone. The underlying symmetry is reflection about the y axis.

The remaining equation now reads

$$\sin\alpha_{+1} - \kappa_d(1 + 4\nu_+)e^{-3\nu_+} = 0, \tag{B7}$$

where $\kappa_d = \frac{n}{2\mathfrak{g}}$.

What we have derived by extremizing the total action with respect to the location of the defect is nothing else but a force balance condition encoding the requirement that in a static baryon configuration the net force must vanish at a defect. It is instructive to see explicitly why it is so. If we take $\mathbf{e}_i$ to be a unit tangent vector at a string end point which represents a force exerted by the i string on the defect, as shown in Fig. 11, then a gravitation force exerted on the defect is to be normalized as $\mathbf{f} = (0, 0, \frac{n}{\mathfrak{g}}(1 + 4\nu_+)e^{-3\nu_+})$.[26] Because there is no net force acting on an object in equilibrium, one has

$$\sum_{i=1}^{2} \mathbf{e}_i + \mathbf{f} = 0. \tag{B8}$$

A solution to the equation for the y component is trivial. It is $e_{y_i} = 0$. Thus, the configuration is effectively two dimensional that allows one to write $\mathbf{e}_1 = (-\cos\alpha_{+1}, 0, -\sin\alpha_{+1})$ and $\mathbf{e}_2 = (\cos\alpha_{+2}, 0, -\sin\alpha_{+2})$. Then, the remaining two equations give $\cos\alpha_{+1} = \cos\alpha_{+2}$ and $\sin\alpha_{+1} = \kappa_d(1 + 4\nu_+)e^{-3\nu_+}$. This is exactly what we have been looking for.

The approach based on the force balance condition is effective and gives a practical recipe for writing the gluing conditions at junctions. It can straightforwardly be extended to include a baryon vertex.

2. Three strings meeting at baryon vertex

At this stage, we consider three Nambu-Goto strings beginning at the heavy quark sources on the boundary and ending on the baryon vertex in the interior, as shown in Fig. 11, on the right. Because the action for the baryon vertex (2.3) is of the form (2.4), with n replaced by m, we may write

---

$$\sum_{i=1}^{3} \mathbf{e}_i + \mathbf{f} = 0, \tag{B9}$$

where $\mathbf{f} = (0, 0, \frac{m}{\mathfrak{g}}(1 + 4\nu_+)e^{-3\nu_+})$.

Let us now consider some examples.

The first example is a configuration in which the quarks are placed at the vertices of an equilateral triangle, as shown in Fig. 2. The symmetry of the problem is the group D_3. Hence, the projection of V onto the xy plane is simply a center of the triangle, and all the tangent angles at V are equal to one another, $\alpha_{+1} = \alpha_{+2} = \alpha_{+3}$. In terms of components, the first two of Eq. (B9) are trivially satisfied, while the third gives

$$\sin\alpha_{+1} = \kappa(1 + 4\nu_+)e^{-3\nu_+}, \tag{B10}$$

with $\kappa = \frac{m}{3\mathfrak{g}}$. We have used that $e_{ri} = -\sin\alpha_{+i}$. It is noteworthy that α_+ may be positive or negative depending on the direction of the gravitational force. Alternatively, one could derive the gluing condition (B10) by varying the total action with respect to the position of the baryon vertex, but this way is longer.

The second example is a collinear configuration of the quarks as shown in Fig. 4, on the right. Like in the case of two quarks, the equation for the y component of (B9) yields a trivial solution $e_{y_i} = 0$, which means that the configuration is two dimensional. Hence, one can choose

$$\mathbf{e}_1 = (-\cos\alpha_{+1}, 0, -\sin\alpha_{+1}),$$
$$\mathbf{e}_2 = (\cos\alpha_{+2}, 0, -\sin\alpha_{+2}),$$
$$\mathbf{e}_3 = (-\cos\alpha_{+3}, 0, -\sin\alpha_{+3}). \tag{B11}$$

Then, the equations for the remaining components become

$$\cos\alpha_{+1} - \cos\alpha_{+2} - \cos\alpha_{+3} = 0,$$
$$\sum_{i=1}^{3} \sin\alpha_{+i} = 3\kappa(1 + 4\nu_+)e^{-3\nu_+}. \tag{B12}$$

Our final example is more complicated, but not by much. Consider a configuration where the quarks are placed at the vertices of an isosceles triangle as shown in Fig. 11. Since the configuration has a reflection symmetry with respect to the y axis, we have $\alpha_{+1} = \alpha_{+2}$. In this case, the unit vectors $\mathbf{e}_i$ are defined as

$$\mathbf{e}_1 = (-\cos\beta\cos\alpha_{+1}, -\sin\beta\cos\alpha_{+1}, -\sin\alpha_{+1}),$$
$$\mathbf{e}_2 = (\cos\beta\cos\alpha_{+1}, -\sin\beta\cos\alpha_{+1}, -\sin\alpha_{+1}),$$
$$\mathbf{e}_3 = (0, \cos\alpha_{+3}, -\sin\alpha_{+3}), \tag{B13}$$

where β is the angle shown in Fig. 11.

The equation for the x component of Eq. (B9) is trivial, while the two others are given by

$$\cos\alpha_{+3} = 2\sin\beta\cos\alpha_{+1},$$

$$2\sin\alpha_{+1} + \sin\alpha_{+3} = 3\kappa(1 + 4\nu_+)e^{-3\nu_+}. \tag{B14}$$

The above examples hopefully make the general idea clear. One writes force balance conditions at junctions and interprets those as the gluing conditions for strings. Moreover, this is a practical way which works for all multistring configurations with an arbitrary number of quark sources.

APPENDIX C: LIMITING CASES

This Appendix collects together some of the formulas which are used to analyze the short distance behavior of the potential in Secs. II–IV.

In the case of the equilateral triangle configuration, we consider Eqs. (2.6) and (2.7). A simple analysis reveals that small L corresponds to small ν. However, rather than using expansions in powers of ν, it is somewhat more convenient to expand L and E in terms of λ. This may be done using the relation

$$\nu = \rho^{\frac{1}{2}}\lambda + (1 - 2\kappa^2 - \rho^{\frac{1}{2}})\lambda^2 + O(\lambda^3), \tag{C1}$$

which follows from Eq. (2.9). Here, $\rho = 1 - \kappa^2$. As a consequence, one can show that the behavior of L and E_{3_Q} near $\lambda = 0$ is given by

$$L(\lambda) = \sqrt{\frac{\lambda}{\mathfrak{s}}}(L_0 + L_1\lambda + O(\lambda^2)),$$

$$E_{3_Q}(\lambda) = \mathfrak{g}\sqrt{\frac{\mathfrak{s}}{\lambda}}(E_0 + E_1\lambda + O(\lambda^2)) + C, \tag{C2}$$

with

$$L_0 = \frac{\sqrt{3}}{4}\mathcal{B}\left(\kappa^2;\frac{1}{2},\frac{3}{4}\right),$$

$$L_1 = \frac{\sqrt{3}}{4}\left(\mathcal{B}\left(\kappa^2;-\frac{1}{2},\frac{3}{4}\right) - \mathcal{B}\left(\kappa^2;-\frac{1}{2},\frac{5}{4}\right)\right.$$

$$\left. - 2\rho^{\frac{1}{4}}|\kappa|^{-1}(1 - 2\kappa^2 - \rho^{\frac{1}{2}})\right), \tag{C3}$$

$$E_0 = 3\kappa\rho^{-\frac{1}{4}} + \frac{3}{4}\mathcal{B}\left(\kappa^2;\frac{1}{2},-\frac{1}{4}\right),$$

$$E_1 = -6\kappa\rho^{\frac{1}{4}} + \frac{3}{4}\mathcal{B}\left(\kappa^2;\frac{1}{2},\frac{1}{4}\right) + \sqrt{3}L_1. \tag{C4}$$

Here, $\mathcal{B}(z;a,b) = B(a,b) + B(z;a,b)$, and $B(z;a,b)$ is the incomplete beta function.

In the case of the symmetric collinear configuration, we consider Eqs. (2.19) and (2.20). Here, it is important to know that if ν goes to zero then the integral (2.19) also goes to zero, and as a consequence, small L corresponds to small ν. As before, we expand L and E_{3_Q} in terms of λ. In this case, Eq. (C1) is replaced by

$$\nu = \zeta\lambda + \left(\zeta^2 - \zeta + \frac{3}{4}\kappa(1 - 3\kappa)\right)\lambda^2 + O(\lambda^3), \tag{C5}$$

with $\zeta = \frac{\sqrt{3}}{2}(1 + 2\kappa - 3\kappa^2)^{\frac{1}{2}}$, as it follows from Eq. (2.22). The behavior of L and E_{3_Q} near $\lambda = 0$ is given by Eq. (C2) but with the coefficients replaced by

$$L_0 = \frac{1}{4}\mathcal{B}\left(1 - \zeta^2;\frac{1}{2},\frac{3}{4}\right),$$

$$L_1 = \frac{1}{4}\left(\mathcal{B}(1 - \zeta^2;-\frac{1}{2},\frac{3}{4}) - \mathcal{B}\left(1 - \zeta^2;-\frac{1}{2},\frac{5}{4}\right)\right.$$

$$\left. + 4\frac{1 - \zeta}{1 - 3\kappa}\zeta^{\frac{3}{2}} - 3\kappa\zeta^{\frac{1}{2}}\right), \tag{C6}$$

$$E_0 = (3\kappa - 1)\zeta^{-\frac{1}{2}} + \frac{1}{2}\mathcal{B}\left(1 - \zeta^2;\frac{1}{2},-\frac{1}{4}\right),$$

$$E_1 = (1 - 6\kappa)\zeta^{\frac{1}{2}} + \frac{1}{2}\mathcal{B}\left(1 - \zeta^2;-\frac{1}{2},\frac{1}{4}\right) + 2L_1. \tag{C7}$$

In the case of the collinear configuration with large L and small l, we consider Eqs. (2.34), (2.44), and (2.45). One important difference between this case and the ones we have discussed so far is that there are now two parameters. We have to analyze the behavior of the corresponding equations in a small region near the point (0,1) in a two-dimensional parameter space (ν, λ_2). A first step in doing so is to choose a path from the point (ν, λ_2) to (0,1). There is an ambiguity in choosing the path. For definiteness, we choose the path $\nu = \varepsilon$ and $1 - \sqrt{\lambda_2} = \varepsilon$, with ε a small parameter. This enables us to have expansions in terms of ε and also control path-dependent terms. Then, the expansions are

$$l = \sqrt{\frac{\nu}{\mathfrak{s}}}(l_0 + l_1\nu) + o(\varepsilon^{\frac{3}{2}}),$$

$$L = \frac{1}{\sqrt{\mathfrak{s}}}(-\ln(1 - \sqrt{\lambda}) + \mathcal{L}_0) - \frac{1}{2}\sqrt{\frac{\nu}{\mathfrak{s}}}l_0 + o(\varepsilon^{\frac{1}{2}}),$$

$$E_{3_Q} = \mathfrak{g}\sqrt{\mathfrak{s}}(-\mathrm{e}\ln(1 - \sqrt{\lambda}) + \mathcal{E}_0) + C$$

$$+ \mathfrak{g}\sqrt{\frac{\mathfrak{s}}{\nu}}(E_0 + E_1\nu) + o(\varepsilon^{\frac{1}{2}}), \tag{C8}$$

where

$$l_0 = \frac{1}{2}\xi^{-\frac{1}{2}}B\left(\xi^2;\frac{3}{4},\frac{1}{2}\right),$$

$$l_1 = \frac{1}{2}\xi^{-\frac{3}{2}}\left(\left(2\xi + \frac{3\kappa-1}{4}\frac{1}{\xi}\right)B\left(\xi^2;\frac{3}{4},-\frac{1}{2}\right) - B\left(\xi^2;\frac{5}{4},-\frac{1}{2}\right)\right),$$

$$\text{(C9)}$$

$$E_0 = 1 + 3\kappa + \frac{1}{2}\xi^{\frac{1}{2}}B\left(\xi^2;-\frac{1}{4},\frac{1}{2}\right),$$

$$E_1 = -1 - 6\kappa + \frac{1}{2}\xi^{-\frac{1}{2}}B\left(\xi^2;\frac{1}{4},\frac{1}{2}\right) + \xi l_1, \qquad \text{(C10)}$$

and

$$\mathcal{L}_0 = \int_0^1 dv\left(2(v^{-4}e^{2(v^2-1)}-1)^{-\frac{1}{2}} - \frac{1}{1-v}\right),$$

$$\mathcal{E}_0 = 2\int_0^1 \frac{dv}{v^2}\left(e^{v^2}(1-v^4e^{2(1-v^2)})^{-\frac{1}{2}} - 1 - v^2 - \frac{ev^2}{2(1-v)}\right).$$

$$\text{(C11)}$$

Here, $\xi = \frac{\sqrt{3}}{2}(1 - 2\kappa - 3\kappa^2)^{\frac{1}{2}}$. In Eq. (C8), we indicate the dependence on ν and λ rather than on ε when no ambiguity arises. Notice that the integrals in Eq. (C11) can be evaluated numerically with the result $\mathcal{L}_0 \approx -0.710$ and $\mathcal{E}_0 \approx -3.431$.

APPENDIX D: MORE ON THE Δ LAW

The goal here is to discuss the relation between the three and two-quark potentials,

$$E_{3_Q}(\mathbf{x}_1, \mathbf{x}_2, \mathbf{x}_3)$$
$$= \frac{1}{2}(E_{Q\bar{Q}}(|\mathbf{x}_{12}|) + E_{Q\bar{Q}}(|\mathbf{x}_{23}|) + E_{Q\bar{Q}}(|\mathbf{x}_{13}|)), \quad \text{(D1)}$$

which is called the Δ law.[27] This relation is valid at least to order α_s^2 in perturbation theory [8] and therefore at very small separations between the quarks. However, it is no longer valid at larger separations, where it is assumed to be replaced by the inequality[28]

$$E_{3_Q}(\mathbf{x}_1, \mathbf{x}_2, \mathbf{x}_3) \geq \frac{1}{2}(E_{Q\bar{Q}}(|\mathbf{x}_{12}|) + E_{Q\bar{Q}}(|\mathbf{x}_{23}|) + E_{Q\bar{Q}}(|\mathbf{x}_{13}|))$$

$$\text{(D2)}$$

that is consistent with the Y law for $E_{3_Q}(\mathbf{x}_1, \mathbf{x}_2, \mathbf{x}_3)$.

A natural question to ask at this point is what kind of relations exist between hybrid potentials. Some relations can be deduced by assuming a factorization in the large-T limit such that

---

$$\langle W_{3_Q}(\mathbf{x}_1, \mathbf{x}_2, \mathbf{x}_3, T)\rangle = \prod_{i>j}^3 \langle W_{Q\bar{Q}}(|\mathbf{x}_{ij}|, T)\rangle^{\frac{1}{2}}. \quad \text{(D3)}$$

This assumption seems reasonable for small $|\mathbf{x}_{ij}|$.

The simplest case to consider is an equilateral triangle configuration. For such a geometry, the factorization equation becomes

$$\langle W_{3_Q}(L, T)\rangle = \langle W_{Q\bar{Q}}(L, T)\rangle^{\frac{3}{2}}, \quad \text{(D4)}$$

with L a triangle's side length. In the limit $T \to \infty$, the expectation values of the Wilson loops are given by

$$\langle W_{3_Q}(L, T)\rangle = \sum_{n=0}^{\infty} B_n(L)e^{-E_{3_Q}^{(n)}(L)T},$$

$$\langle W_{Q\bar{Q}}(L, T)\rangle = \sum_{n=0}^{\infty} M_n(L)e^{-E_{Q\bar{Q}}^{(n)}(L)T}. \quad \text{(D5)}$$

For our purposes, it is sufficient to consider the first three energy levels. In that case, Eq. (D4) can be easily solved. First, we assume that $E_{3_Q}^{(n+1)} > E_{3_Q}^{(n)}$ and $E_{Q\bar{Q}}^{(n+1)} > E_{Q\bar{Q}}^{(n)}$ hold in the range of small L. In other words, the energy levels are separated from each other. In addition, we assume that gaps are subject to the constraint $\Delta E_{Q\bar{Q}}^{(2)} < 2\Delta E_{Q\bar{Q}}^{(1)}$, where $\Delta E_{Q\bar{Q}}^{(i)} = E_{Q\bar{Q}}^{(i)} - E_{Q\bar{Q}}^{(0)}$. The factorization equation is then simply

$$B_0 e^{-E_{3_Q}^{(0)}T} + B_1 e^{-E_{3_Q}^{(1)}T} + B_2 e^{-E_{3_Q}^{(2)}T}$$
$$= M_0^{\frac{3}{2}}e^{-\frac{3}{2}E_{Q\bar{Q}}^{(0)}T}\left(1 + \frac{3M_1}{2M_0}e^{-\Delta E_{Q\bar{Q}}^{(1)}T} + \frac{3M_2}{2M_0}e^{-\Delta E_{Q\bar{Q}}^{(2)}T}\right),$$

$$\text{(D6)}$$

modulo terms decaying faster as $T \to \infty$. Equating order by order the two sides of the equation gives

$$E_{3_Q}^{(0)}(L) = \frac{3}{2}E_{Q\bar{Q}}^{(0)}(L), \qquad E_{3_Q}^{(i)}(L) = \frac{1}{2}E_{Q\bar{Q}}^{(0)}(L) + E_{Q\bar{Q}}^{(i)}(L).$$

$$\text{(D7)}$$

The first equation is nothing but the Δ law, whereas the second is its generalization to excited levels. In practice [25], the assumptions we made are valid if $L < 0.7$ fm. In that case, $E_{Q\bar{Q}}^{(1)}$ corresponds to the Π_u hybrid potential, and $E_{Q\bar{Q}}^{(2)}$ corresponds to the Σ_u^- one.

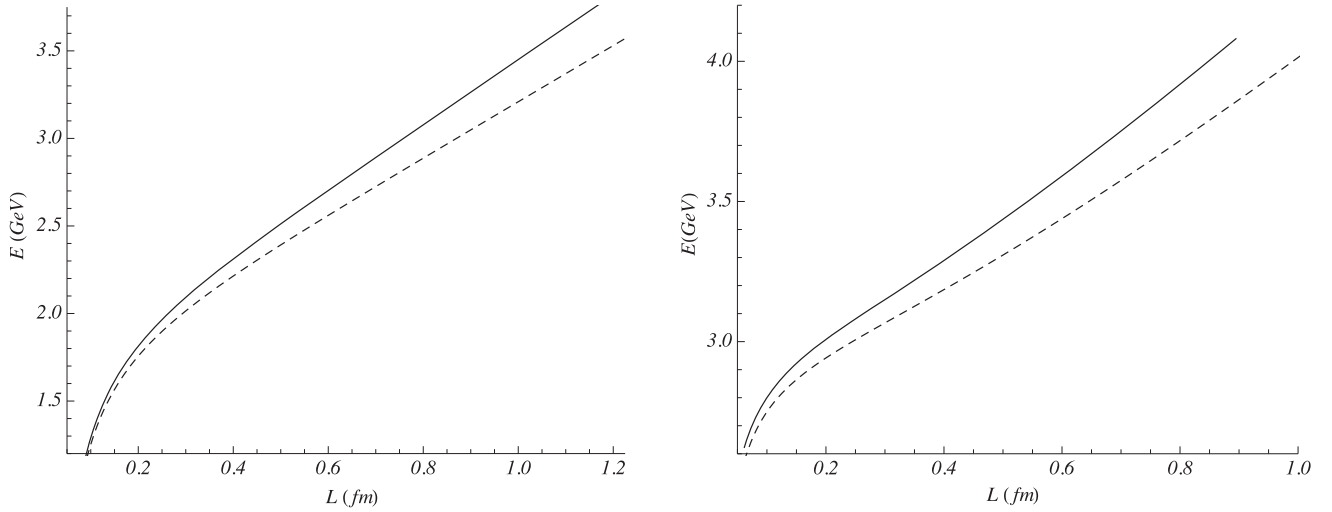At this point, we should mention that for large L the Y law suggests the inequalities

FIG. 12. Left: E_{3_Q} (solid curve) and $\frac{3}{2}E_{Q\bar{Q}}$ (dashed curve). Right: $\tilde{E}_{3_Q}$ (solid curve) and $\frac{1}{2}E_{Q\bar{Q}} + \tilde{E}_{Q\bar{Q}}$ (dashed curve). In both cases, we set $\mathfrak{g} = 0.176$, $\mathfrak{s} = 0.44$ GeV^2, $\kappa = -0.083$, $\kappa_d = 1300$, and $C = 1.87$ GeV. $E_{Q\bar{Q}}$ and $\tilde{E}_{Q\bar{Q}}$ are from Refs. [22] and [26], respectively.

$$E_{3_Q}^{(0)}(L) \geq \frac{3}{2}E_{Q\bar{Q}}^{(0)}(L), \qquad E_{3_Q}^{(i)}(L) \geq \frac{1}{2}E_{Q\bar{Q}}^{(0)}(L) + E_{Q\bar{Q}}^{(i)}(L).$$

$$(D8)$$

These, in turn, suggest the following inequalities between meson and baryon masses:

$$2M(QQQ) \geq 3M(Q\bar{Q}),$$
$$2M(QQQg) \geq M(Q\bar{Q}) + 2M(Q\bar{Q}g). \qquad (D9)$$

While the first is known in the literature [2], the second is new. It involves the masses of hybrids.

As a final comment, we note that the model we are considering allows us to check two of these inequalities numerically. Figure 12 shows the results for the ground states and excited states corresponding to the Σ excitation. Obviously, the three-quark potentials can be approximated by a set of the two-quark potentials only at short distances.

APPENDIX E: ANOTHER CALCULATION OF THE QUARK-QUARK POTENTIAL

Here, we will carry out a calculation of the static quark-quark potential using the same geometry as that of Ref. [36]. The result will be equivalent to what we had before. This provides more evidence that the potential (3.8) is geometry independent.

Consider a geometry in which the quarks are at the vertices of an isosceles triangle. We are interested in the limiting case when the base length l is much smaller than the triangle's height L, as shown in Fig. 13. Since the configuration has a reflection symmetry with respect to the y axis, the side strings have an identical profile, and the projection of V on the xy plane lies on the y axis. Notice

that α_1 is positive. This can be understood as follows. Consider a configuration similar to the one shown in Fig. 7 such that Q_3 lies on the x axis. Obviously, one can smoothly move Q_3 to the y axis along a circle of radius L. In the limit $l \to 0$ and $L \to \infty$, this may not lead to a radical change of the string's profiles.

Given this, we can use the general formula (A6) to write the distance between the points Q_1 and O via an integral,

$$l_1 = \cos\alpha_1 \sqrt{\frac{\nu}{\mathfrak{s}}} \int_0^1 dv_1 v_1^2 e^{\nu(1-v_1^2)} (1 - \cos^2\alpha_1 v_1^4 e^{2\nu(1-v_1^2)})^{-\frac{1}{2}}.$$

$$(E1)$$

In a similar fashion, Eq. (A16) tells us how to do so for the distance between the points Q_3 and O. Here, we have
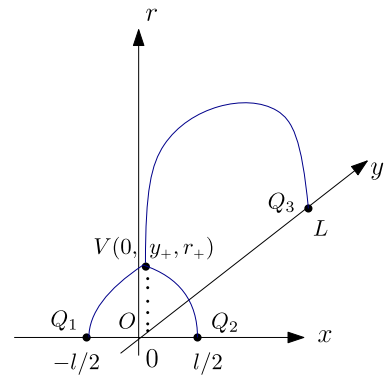

FIG. 13. A baryon configuration for $L \gg l$. The quarks Q_i are placed at the vertices of the isosceles triangle. V is the vertex, and O is its projection on the y axis.

$$l_3 = \sqrt{\frac{\lambda}{\mathfrak{s}}} \left[\int_0^1 dv_3 v_3^2 e^{\lambda(1-v_3^2)} (1 - v_3^4 e^{2\lambda(1-v_3^2)})^{-\frac{1}{2}} \right.$$
$$\left. + \int_{\sqrt{\frac{\xi}{\lambda}}}^1 dv_3 v_3^2 e^{\lambda(1-v_3^2)} (1 - v_3^4 e^{2\lambda(1-v_3^2)})^{-\frac{1}{2}} \right], \quad \text{(E2)}$$

with $\frac{e^\lambda}{\lambda} = \frac{e^\nu}{\nu} \cos \alpha_3$. If β is a base angle of the isosceles triangle $Q_1 Q_2 O$, then a simple geometric analysis leads to

$$l = 2 \cos \beta l_1, \qquad L = \sin \beta l_1 + l_3. \quad \text{(E3)}$$

The energies of the two first strings can be read from Eq. (A9), while that of the third can be read from Eq. (A20). Combining those with Eq. (2.3) for the gravitational energy of the vertex, we find the total energy of the configuration

$$E_{3_Q} = \mathfrak{g} \sqrt{\frac{\mathfrak{s}}{\nu}} \left[3\kappa e^{-2\nu} \right.$$
$$\left. + 2 \int_0^1 \frac{dv_1}{v_1^2} (e^{\nu v_1^2} (1 - \cos^2 \alpha_1 v_1^4 e^{2\nu(1-v_1^2)})^{-\frac{1}{2}} - 1 - v_1^2) \right]$$
$$+ C + \mathfrak{g} \sqrt{\frac{\mathfrak{s}}{\lambda}} \left[\int_0^1 \frac{dv_3}{v_3^2} (e^{\lambda v_3^2} (1 - v_3^4 e^{2\lambda(1-v_3^2)})^{-\frac{1}{2}} \right.$$
$$\left. - 1 - v_3^2) + \int_{\sqrt{\frac{\xi}{\lambda}}}^1 \frac{dv_3}{v_3^2} e^{\lambda v_3^2} (1 - v_3^4 e^{2\lambda(1-v_3^2)})^{-\frac{1}{2}} \right]. \quad \text{(E4)}$$

To complete the picture, we would need the gluing conditions at the vertex to show that the three-quark potential is written parametrically as $E_{3_Q} = E(\nu, \lambda)$, $l = l(\nu, \lambda)$, and $L = L(\nu, \lambda)$. These conditions include two equations for force equilibrium, in the y and r directions. From Eq. (B14), it follows that

$$\cos \alpha_3 = 2 \sin \beta \cos \alpha_1,$$
$$2 \sin \alpha_1 + \sin \alpha_3 = 3\kappa(1 + 4\nu)e^{-3\nu}. \quad \text{(E5)}$$

Notice that α_3 is negative.

Just as in the case of the collinear configuration with large L and small l, we have to analyze the behavior of the parametric equations in a small region near the point $(0,1)$ in a two-dimensional parameter space (ν, λ). To this end, we choose the path $\nu = \varepsilon$ and $1 - \sqrt{\lambda} = \varepsilon$ that enables us to have expansions in terms of ε and control path-dependent terms. A straightforward but somewhat tedious calculation shows that

$$l = \sqrt{\frac{\nu}{\mathfrak{s}}} (l_0 + l_1 \nu) + o(\epsilon^{\frac{3}{2}}),$$
$$L = \frac{1}{\sqrt{\mathfrak{s}}} (-\ln(1 - \sqrt{\lambda}) + \mathcal{L}_0) + o(\epsilon^{\frac{1}{2}}),$$
$$E_{3_Q} = \mathfrak{g}\sqrt{\mathfrak{s}}(-e \ln(1 - \sqrt{\lambda}) + \mathcal{E}_0) + C$$
$$+ \mathfrak{g}\sqrt{\frac{\mathfrak{s}}{\nu}} (E_0 + E_1 \nu) + o(\epsilon^{\frac{1}{2}}), \quad \text{(E6)}$$

with the same l_i's, $\mathcal{L}_0$, $\mathcal{E}_0$, and E_i's as in Eqs. (C9)–(C11). As before, we indicate the dependence on ν and λ rather than on ε when no ambiguity arises.

Finally, we reduce the parametric equations to a single one,

$$E_{3_Q}(l, L) = -\frac{\alpha_{QQ}}{l} + \sigma_0 l + \sigma L + c + o(l), \quad \text{(E7)}$$

with the same α_{QQ}, σ_0, σ, and c as in Eq. (3.6).

As in Sec. III, we have to be careful in extracting the quark-quark potential from the above expression. In the limit we are considering, the y coordinate of the vertex behaves like $y_+ \sim \varepsilon^{\frac{3}{2}} \sim l^3$. This means that to the approximation we are using the projection of V is located at the origin. In contrast, from the four-dimensional perspective, it should be located at $y = l/2\sqrt{3}$ [36]. Thus, we have to subtract from E_{3_Q} the term proportional to σ and a constant term. As a result, we arrive at the expression (3.8).

[1] J. D. Bjorken, Report No. FERMILAB-Conf-85/69, 1985.
[2] J.-M. Richard, Phys. Rep. **212**, 1 (1992); Nucl. Phys. **A752**, 129 (2005); arXiv:1205.4326.
[3] J. M. Cornwall, Nucl. Phys. **B128**, 75 (1977); Phys. Rev. D **54**, 6527 (1996).
[4] X. Artru, Nucl. Phys. **B85**, 442 (1975).
[5] N. Isgur and J. Paton, Phys. Rev. D **31**, 2910 (1985).
[6] J. M. Cornwall, Phys. Rev. D **69**, 065013 (2004).
[7] J. Vijande, A. Valcarce, and H. Garcilazo, Phys. Rev. D **90**, 094004 (2014).
[8] G. S. Bali, Phys. Rep. **343**, 1 (2001).
[9] T. T. Takahashi, H. Suganuma, Y. Nemoto, and H. Matsufuru, Phys. Rev. D **65**, 114509 (2002).
[10] C. Alexandrou, Ph. de Forcrand, and O. Jahn, Nucl. Phys. B, Proc. Suppl. **119**, 667 (2003).
[11] N. Sakumichi and H. Suganuma, Phys. Rev. D **92**, 034511 (2015).
[12] C. Alexandrou, Ph. de Forcrand, and A. Tsapalis, Phys. Rev. D **65**, 054503 (2002).
[13] Y. Koma and M. Koma, Proc. Sci., LATTICE2014 (2014) 352.
[14] T. T. Takahashi and H. Suganuma, Phys. Rev. D **70**, 074506 (2004).

[15] C. A. Meyer and E. S. Swanson, Prog. Part. Nucl. Phys. **82,** 21 (2015).

[16] J. Maldacena, Adv. Theor. Math. Phys. **2,** 231 (1998).

[17] O. Andreev, Phys. Rev. D **78,** 065007 (2008).

[18] O. Andreev, Phys. Lett. B **756,** 6 (2016).

[19] A. Karch, E. Katz, D. T. Son, and M. A. Stephanov, Phys. Rev. D **74,** 015005 (2006).

[20] O. Andreev, Phys. Rev. D **73,** 107901 (2006).

[21] O. Aharony, S. S. Gubser, J. M. Maldacena, H. Ooguri, and Y. Oz, Phys. Rep. **323,** 183 (2000).

[22] O. Andreev and V. I. Zakharov, Phys. Rev. D **74,** 025023 (2006).

[23] C. D. White, Phys. Lett. B **652,** 79 (2007).

[24] M. V. Carlucci, F. Giannuzzi, G. Nardulli, M. Pellicoro, and S. Stramaglia, Eur. Phys. J. C **57,** 569 (2008).

[25] K. J. Juge, J. Kuti, and C. Morningstar, Phys. Rev. Lett. **90,** 161601 (2003).

[26] O. Andreev, Phys. Rev. D **86,** 065013 (2012); **87,** 065006 (2013).

[27] E. Witten, J. High Energy Phys. 07 (1998) 006.

[28] D. J. Gross and H. Ooguri, Phys. Rev. D **58,** 106002 (1998).

[29] O. Andreev, Phys. Rev. D **76,** 087702 (2007).

[30] B. M. Barbashov and V. V. Nesterenko, *Introduction to the Relativistic String Theory* (World Scientific, Singapore, 1990).

[31] See, e. g., https://reference.wolfram.com/language/ref/Product Log.html.

[32] J. M. Maldacena, Phys. Rev. Lett. **80,** 4859 (1998).

[33] M. J. Savage and M. B. Wise, Phys. Lett. B **248,** 177 (1990).

[34] D. Ebert, R. N. Faustov, V. O. Galkin, and A. P. Martynenko, Phys. Rev. D **66,** 014008 (2002).

[35] O. W. Greenberg and H. J. Lipkin, Nucl. Phys. **A370,** 349 (1981).

[36] C. Alexandrou, Ph. de Forcrand, and B. Lucini, Phys. Rev. Lett. **97,** 222002 (2006).

[37] G. S. Bali and A. Pineda, Phys. Rev. D **69,** 094001 (2004).

[38] A. Athenodorou, B. Bringoltz, and M. Teper, J. High Energy Phys. 02 (2011) 030; S. Dubovsky, R. Flauger, and V. Gorbenko, J. Exp. Theor. Phys. **120,** 399 (2015).

[39] M. Caselle, G. Delfino, P. Grinza, O. Jahn, and N. Magnoli, J. Stat. Mech. 0603, P03008 (2006).

[40] Ph. de Forcrand and O. Jahn, Nucl. Phys. B, Proc. Suppl. **129,** 700 (2004); Nucl. Phys. **A755,** 475 (2005).

[41] N. Brambilla, J. Ghiglieri, and A. Vairo, Phys. Rev. D **81,** 054031 (2010).

[42] See, e. g., L. Randall and R. Sundrum, Phys. Rev. Lett. **83,** 3370 (1999); C. P. Burgess, F. Quevedo, S. J. Rey, G. Tasinato, and I. Zavala, J. High Energy Phys. 10 (2002) 028.

[43] R. R. Metsaev and A. A. Tseytlin, Nucl. Phys. **B533,** 109 (1998).

[44] A. M. Polyakov, *Gauge Fields and Strings* (Harwood, Academnic, Chur, Switzerland, 1987).

[45] O. Andreev, Phys. Rev. Lett. **102,** 212001 (2009).

[46] C. Athanasiou, H. Liu, and K. Rajagopal, J. High Energy Phys. 05 (2008) 083.